

PM/97-25
 UFR-HEP/98-09
 August 1998

Radiative corrections to $e^+e^- \rightarrow H^+H^-$: THDM versus MSSM .

A. Arhrib^{a,b¶}, G. Moultaka^{c||}

*a: Département de Mathématiques, Faculté des Sciences et Techniques,
 B.P 416 Tanger Morocco*

*b: UFR-Physique des Hautes Energies, Faculté des Sciences
 PO Box 1014, Rabat-Morocco*

*c: Laboratoire de Physique Mathématique et Théorique, CNRS-UMR 5825
 Université Montpellier II, F-34095 Montpellier Cedex 5, France*

Abstract

One loop radiative corrections to $e^+e^- \rightarrow H^+H^-$ are considered at future linear collider energies, in the general type II Two Higgs Doublet Model (THDM) and in the Minimal Supersymmetric Standard Model-like (MSSM) Higgs sector. To make the comparison between THDM and MSSM tractable, we have introduced a quasi-SUSY parameterization which preserves all the tree-level Higgs mass-sum-rules of the MSSM, and involves just 3 free parameters in the Higgs sector (instead of 7 in the general THDM) and comprises the MSSM as a particular case. The model-independent soft photon contribution is isolated and shown to be substantial. Important effects come also from the contribution of the model dependent $h^0H^+H^-$ and $H^0H^+H^-$ vertices to the final state. In the MSSM, the contribution of the Higgs sector is moderate (a few percent) while in the THDM and both for small and large $\tan\beta$ important effects ($\sim +30\%$) can be found.

¶E-mail:arhrib@fstt.ac.ma

||E-mail:moultaka@lpm.univ-montp2.fr

1 Introduction

Supersymmetry is one of the most promising scenarios in terms of which one can approach new physics at the present and next generation of colliders (LEP II, upgraded CDF, LHC, LC2000,...). In this context, the awaited discovery of a neutral Higgs particle, if successful, will need to be complemented by the discovery and study of the full-fledged Higgs sector as well as the purely supersymmetric sector, in order to test unambiguously the Minimal Supersymmetric Standard Model (MSSM) [1] or possibly its non-minimal extensions [2].

Such a task will presumably be rather intricate as any realistic supersymmetric model predicts a plethora of particles and associated couplings. It should also comprise a full test of the various mass-sum-rules and relations among the couplings endemic to supersymmetry [3], these being, in some cases, sensibly modified by radiative corrections [4, 5].

These large modifications can be crucial in the experimental search strategy. Perhaps the most illustrative example is the loosening of the MSSM tree-level mass bound for the lightest CP-even Higgs roughly from

$$m_{h^0}^2 \leq M_Z^2 \quad \text{to} \quad m_{h^0}^2 \lesssim M_Z^2 + g^2 \frac{3m_t^4}{8\pi^2 M_W^2} \ln\left(\frac{m_t^2}{m_t^2}\right)$$

by loop effects [4, 5], which raises the mass bound to ~ 130 GeV below which the lightest Higgs should be discovered or else the MSSM ruled out.

Sizeable modifications of tree-level predictions are likely to occur not only in the Higgs mass-sum-rules[6] but also in Higgs self-couplings, and more moderately in mass relations and couplings in the chargino, neutralino, squark, slepton and gluino sectors. Some of these have been already looked at [7] in a model dependent context, however ultimately a systematic exploration of all regions of susy parameters leading to potentially large deviations that can affect tree level relations as well as production and decay rates of new particles, would become mandatory in order to achieve full tests of susy. Indeed there is *a priori* no guarantee that moderate corrections to a given observable will ensure moderate corrections to all other observables related to the same given sector.

The subject of the present paper is the one-loop electroweak corrections to the charged Higgs pair production in e^+e^- collisions. This will turn out to be precisely an example where important effects are present in the production cross-section, even though corrections to the H^\pm mass sum rule are known to be modest [8]. (Loop corrections to H^\pm decays are also important to study [9] but will not be considered in this paper).

Generally speaking, a charged scalar particle coupled to fermions proportionally to their masses is a by-product of an extended Higgs sector with scalar fields in non-singlet representations of the weak symmetry. As such its experimental discovery would thus be immediate qualitative evidence in favor of a structure beyond the standard model, in contrast with the neutral Higgs which would necessitate a more quantitative investigation. Present experimental direct search for charged Higgses set lower bound on its mass. At LEP-II search, ALEPH and OPAL Collaborations set a lower bound of 52 GeV and DELPHI Collaboration sets a lower bound of 54.4 GeV [10]. At the Tevatron, CDF collaboration has searched for charged Higgs decay of the top quark excluding a charged Higgs

mass lower than ~ 147 GeV in the large $\tan\beta$ limit [11]. However, using the Tevatron quark data in the lepton plus τ a lower mass limit of 100 GeV for $\tan\beta \geq 40$ has been reported [12]. For a recent discussion of the LEP and Tevatron limits and a reappraisal see [13]

Indirect limits, valid only in the non supersymmetric case, have been inferred from $b \rightarrow s\gamma$ and read [14]:

$$M_{H^\pm} > 244\text{GeV} + \frac{63}{\tan\beta^{1.3}}\text{GeV}$$

see also [15].

Although supersymmetry can generically invalidate the previous indirect limit, some studies suggest that useful bounds can still be inferred in some model-dependent cases (assuming grand unified minimal supergravity and a negative Higgs mass parameter μ [16]). At hadronic machines, future direct production of charged Higgses can proceed either via pair production through gluon-gluon fusion [17] or the less favoured $q\bar{q}$ annihilation Drell-Yan process[18], or via single production in association with quarks[19] or a W boson[20]. On the other hand, the charged Higgs can be efficiently searched for only when its top-bottom decay mode is kinematically forbidden [otherwise one would have to look at bosonic decay modes ex. $H^\pm \rightarrow h^0 W^\pm$, $H^\pm \rightarrow A^0 W^\pm$, [18], see also [13]].

The future e^+e^- machines will presumably offer a cleaner environment and in that sense a higher mass reach, especially if the 1–2TeV options are available. There the charged Higgs can be produced either in pairs through γ, Z exchange[21], or in single rare production in association with a W boson [22]. The former channel has at tree-level the particularity of depending only on standard model parameters, it is thus important to understand the trend of loop effects which contain the model dependence.

The one-loop electroweak corrections to $e^+e^- \rightarrow H^+H^-$ have been previously considered at NLC energies, restricting mainly to top-bottom, squarks and sleptons contributions [23]. In the present paper we complete the study by including the effects of the remaining sectors already summarized in. We also revise some of the numerical results previously given in [23]. We mention here incidently that charged Higgs pair production through laser back-scattered $\gamma\gamma$ collisions has been studied in the literature at the tree as well as the one-loop levels [25] reaching similar conclusions as to the importance of the quantum corrections.

In view of the potentially large corrections the first issue here will be mainly (but not exclusively), to pin down all possible large effects from other sectors than the ones considered in [23]. For this we present the full set of one-loop corrections in a general type II two-Higgs-doublet model (THDM-II), that is the complete Higgs sector contributions (self-energies, vertices and boxes), the infrared part including initial and final soft photon radiation, $\gamma\gamma$, γZ and WW boxes, as well as the (standard) initial state vertex and fermion and gauge boson self-energies contributions. THDM-II, besides being interesting in its own right, is a relevant framework in terms of which to assess the sensitivity to supersymmetric effects.

The second issue will be to parameterize the comparison between THDM-II and the more constrained MSSM cases. Indeed it will turn out that apart from large model independent contributions in the infrared sector, important effects are found in diagrams involving triple Higgs couplings, however only in the non-supersymmetric case. In order to assess the sensitivity to such effects it will be appropriate to define an effective parameterization where all the (tree-level) MSSM Higgs mass-sum-rules remain valid while some of the tree-level triple Higgs couplings deviate from their MSSM form. This parameterization which we will dub “quasi-supersymmetric” necessitates just one extra free parameter (instead of five) in the Higgs sector, as compared to the MSSM and actually offers a general setting to quantify the tests of the self-couplings in the Higgs sector.

The rest of the paper is organized as follows. In section II we review the main features of the Higgs potential in THDM-II as well as in the MSSM. We then define and discuss the “quasi-supersymmetric” parameterization which interpolates between the two models and recall the form of the various Higgs couplings. In section III the tree-level production cross-section is presented and some notations and conventions defined. Section IV is devoted to the general form of the radiative corrections and to a description of the various contributions. In section V we describe the renormalization scheme which is most suited in our case to a comparison between the supersymmetric and non-supersymmetric cases, and discuss as well the Infrared sector. Section VI is devoted to the numerical analysis, and section VII to the conclusion. Finally, presentation of complementary analytic expressions and technical details of the calculation is relegated to the appendices.

2 The relevant Lagrangian and the “quasi-susy” parameterization.

In this section we focus on the structure of the charged Higgs couplings to the other Higgs fields and recall as well its couplings to the gauge bosons and matter fermions, excluding the supersymmetric sector. We will refrain from presenting extensively the various features of the Higgs potential, as this has been repeatedly achieved in the literature ¹ The aim here is rather to identify the tree-level couplings which can carry information about the presence of supersymmetry, distinguishing them from those which have the same form whether susy is operative or not. We then encompass these features in a suitable general parameterization.

2.1 The two-Higgs doublet potential

Assuming two complex $SU(2)_{weak}$ doublet scalar fields Φ_1 and Φ_2 defined as

¹we follow throughout this section the notations of [26] to which we refer the reader for relevant details

$$\Phi_1 = \begin{pmatrix} \phi_1^+ = \varphi_1 + i\varphi_2 \\ \phi_1^0 = \varphi_3 + i\varphi_4 \end{pmatrix} \quad \Phi_2 = \begin{pmatrix} \phi_2^+ = \varphi_5 + i\varphi_6 \\ \phi_2^0 = \varphi_7 + i\varphi_8 \end{pmatrix}$$

the most general (dimension 4) $SU(2)_{weak} \times U(1)_Y$ gauge invariant and (CP-invariant) scalar potential is given by (see, however, the Errata in ref [26]):

$$\begin{aligned} V(\Phi_1, \Phi_2) = & \lambda_1(\Phi_1^+ \Phi_1 - v_1^2)^2 + \lambda_2(\Phi_2^+ \Phi_2 - v_2^2)^2 + \lambda_3((\Phi_1^+ \Phi_1 - v_1^2) + (\Phi_2^+ \Phi_2 - v_2^2))^2 \\ & + \lambda_4((\Phi_1^+ \Phi_1)(\Phi_2^+ \Phi_2) - (\Phi_1^+ \Phi_2)(\Phi_2^+ \Phi_1)) + \lambda_5(Re(\Phi_1^+ \Phi_2) - v_1 v_2)^2 + \\ & \lambda_6 Im(\Phi_1^+ \Phi_2)^2 + \lambda_7 \end{aligned} \quad (1)$$

where Φ_1 and Φ_2 have weak hypercharge $Y=1$ and the λ_i 's are real-valued. We will also assume the arbitrary additive constant λ_7 to be vanishing. This would of course be the case if exact supersymmetry is imposed, and should any way be required for a vanishing cosmological constant (at least as a tree-level approximation). No other assumptions on the λ_i 's are made except that they sit in the regions that allow the required pattern of spontaneous electroweak symmetry breaking down to $U(1)_{ew}$ [27].

The minimum of the potential is then obtained for

$$\langle \Phi_1 \rangle = \begin{pmatrix} v_1 \\ 0 \end{pmatrix} \quad \langle \Phi_2 \rangle = \begin{pmatrix} v_2 \\ 0 \end{pmatrix}$$

After the Higgs mechanism has taken place, the W and Z gauge bosons acquire masses given by $m_W^2 = \frac{1}{2}g^2 v^2$ and $m_Z^2 = \frac{1}{2}(g^2 + g'^2)v^2$, where g and g' are the $SU(2)_{weak}$ and $U(1)_Y$ gauge couplings and $v^2 = v_1^2 + v_2^2$. The combination $v_1^2 + v_2^2$ is thus fixed by the electroweak scale through $v_1^2 + v_2^2 = (2\sqrt{2}G_F)^{-1}$ and we are left with 7 free parameters in eq.(1), namely the λ_i 's and v_2/v_1 .

On the other hand, three of the eight degrees of freedom of the two Higgs doublets correspond to the 3 goldstone bosons, the remaining five become the physical Higgs bosons H^0, h^0 (CP-even), A^0 (CP-odd) and H^\pm . Their masses are obtained as usual from the shift $\Phi_i \rightarrow \Phi_i + \langle \Phi_i \rangle$ and read

$$m_{A^0}^2 = \lambda_6 v^2; \quad m_{H^\pm}^2 = \lambda_4 v^2 \quad \text{and} \quad m_{H^0, h^0}^2 = \frac{1}{2}[A + C \pm \sqrt{(A - C)^2 + 4B^2}] \quad (2)$$

where

$$A = 4v_1^2(\lambda_1 + \lambda_3) + v_2^2\lambda_5, \quad B = v_1 v_2(4\lambda_3 + \lambda_5) \quad \text{and} \quad C = 4v_2^2(\lambda_2 + \lambda_3) + v_1^2\lambda_5 \quad (3)$$

The angle β given by $\tan \beta = v_2/v_1$ defines the mixing leading to the physical H^\pm and A^0 states, while the mixing angle α associated to H^0, h^0 physical states is given by [See ref [26] for further details.]

$$\sin 2\alpha = \frac{2B}{\sqrt{(A - C)^2 + 4B^2}}, \quad \cos 2\alpha = \frac{A - C}{\sqrt{(A - C)^2 + 4B^2}} \quad (4)$$

It will be more suitable for the forthcoming discussion to trade the five parameters $\lambda_{1,2,4,5,6}$ for the 4 Higgs masses and the mixing angle α . From now on we will take the physical Higgs masses, $m_{H^0}, m_{h^0}, m_{A^0}, m_{H^\pm}$, the mixing angles α, β and the coupling λ_3 as the 7 free parameters.

It is then straightforward algebra to invert equations (2) through (4), and get the λ_i 's in terms of this new set of parameters.

$$\lambda_4 = \frac{g^2}{2m_W^2} m_{H^\pm}^2 \quad \lambda_6 = \frac{g^2}{2m_W^2} m_A^2 \quad (5)$$

$$\lambda_5 = \frac{g^2}{2m_W^2} \frac{\sin 2\alpha}{\sin 2\beta} (m_H^2 - m_h^2) - 4\lambda_3 \quad (6)$$

$$\lambda_1 = \frac{g^2}{16 \cos^2 \beta m_W^2} [m_H^2 + m_h^2 + (m_H^2 - m_h^2) \frac{\cos(2\alpha + \beta)}{\cos \beta}] + \lambda_3 (-1 + \tan^2 \beta) \quad (7)$$

$$\lambda_2 = \frac{g^2}{16 \sin^2 \beta m_W^2} [m_H^2 + m_h^2 + (m_h^2 - m_H^2) \frac{\sin(2\alpha + \beta)}{\sin \beta}] + \lambda_3 (-1 + \cot^2 \beta) \quad (8)$$

Using the above expressions, and after having expressed eq.(1) in terms of the Goldstone and physical Higgs fields, one can cast all couplings of the scalar potential in terms of the new set of free parameters.

Here we restrict ourselves to all 3-point vertices (see eqs. (A.1–A.5) of appendix A) involving a charged Higgs field, since these are the only ones that enter one-loop calculations in $e^+e^- \rightarrow H^+H^-$ (4-point vertices involving H^\pm have vanishing contributions). Injecting eq.(5–8) in eqs. (A.1–A.5) we get the various couplings in terms of the new set of free parameters,

$$g_{H^0 H^+ H^-} = -i \frac{g}{m_W} [\cos(\beta - \alpha) (m_{H^\pm}^2 - \frac{m_H^2}{2}) + \frac{\sin(\alpha + \beta)}{\sin 2\beta} \{4\lambda_3 v^2 + \frac{1}{2}(m_H^2 + m_h^2) - \frac{1}{2 \sin 2\beta} (\sin 2\alpha + 2 \sin(\alpha - \beta) \cos(\alpha + \beta)) (m_H^2 - m_h^2)\}] \quad (9)$$

$$g_{h^0 H^+ H^-} = -i \frac{g}{m_W} [\sin(\beta - \alpha) (m_{H^\pm}^2 - \frac{m_h^2}{2}) + \frac{\cos(\alpha + \beta)}{\sin 2\beta} \{4\lambda_3 v^2 + \frac{1}{2}(m_H^2 + m_h^2) - \frac{1}{2 \sin 2\beta} (\sin 2\alpha + 2 \sin(\alpha + \beta) \cos(\alpha - \beta)) (m_H^2 - m_h^2)\}] \quad (10)$$

$$g_{H^0 H^\pm G^\mp} = \frac{-ig \sin(\beta - \alpha) (m_{H^\pm}^2 - m_H^2)}{2m_W} \quad (11)$$

$$g_{h^0 H^\pm G^\mp} = \frac{ig \cos(\beta - \alpha) (m_{H^\pm}^2 - m_h^2)}{2m_W} \quad (12)$$

$$g_{A^0 H^\pm G^\mp} = \mp \frac{v}{\sqrt{2}} (\lambda_6 - \lambda_4) = \mp \frac{m_{H^\pm}^2 - m_A^2}{v\sqrt{2}} \quad (13)$$

It is noteworthy that λ_3 enters only $g_{H^0 H^+ H^-}$ and $g_{h^0 H^+ H^-}$ while $g_{H^0 H^\pm G^\mp}, g_{h^0 H^\pm G^\mp}$ and $g_{A^0 H^\pm G^\mp}$ have automatically their MSSM form, however, without assuming the MSSM mass-sum-rules. As we will see in the next subsection, a direct consequence when MSSM

mass-sum-rules are assumed, will be that λ_3 measures the “amount” of “hard” susy breaking, and that among the five couplings, only $g_{H^0 H^+ H^-}$ and $g_{h^0 H^+ H^-}$ are sensitive to such a breaking. We should also stress that no constraint has been imposed thus far, in the derivation of the preceding expressions. In particular no sign assignments for the trigonometric functions of α or β where made (apart of course from the definition $\tan \beta \equiv v_2/v_1 > 0$)

2.2 The “quasi-susy” parameterization

We proceed hereafter to the definition of a partly constrained parameterization which interpolates between the free THDM case, and the constrained MSSM, in the following sense:

- a) It preserves *all* tree-level mass-sum-rules of the MSSM, including the relation between $\tan 2\alpha$ and $\tan 2\beta$ ²;
- b) It needs just 3 free parameters (instead of 7) and comprises the susy case as a special case with 2 free parameters;

Actually such a parameterization would be phenomenologically very natural in case where more than one Higgs particle is discovered, with masses consistent with the MSSM sum-rules. Indeed, taking these sum-rules as granted, one can devise a strategy for further precision tests of the supersymmetric self-Higgs couplings, where a reduced number of free parameters is involved and particularly sensitive sectors are identified .

Let us first recall the situation when softly broken supersymmetry is imposed in eq.(1). As shown in [26] one has the following relations among the λ_i ’s:

$$\begin{aligned} \lambda_1 = \lambda_2 \quad , \quad \lambda_3 = \frac{1}{8}(g^2 + g'^2) - \lambda_1 \quad , \quad \lambda_4 = 2\lambda_1 - \frac{1}{2}g'^2 \\ \lambda_5 = -\frac{1}{2}(g^2 + g'^2) + 2\lambda_1 \quad , \quad \lambda_6 = -\frac{1}{2}(g^2 + g'^2) + 2\lambda_1 \end{aligned} \quad (14)$$

Due to these five constraints one is left with two free parameters, ex. $\tan \beta$ and m_A . It should be stressed that the soft breaking, in the Higgs sector, is actually encoded in this two-parameter freedom. (Indeed, if exact susy were imposed, $V_{soft} = 0$, then all λ_i ’s would be fixed in terms of the gauge couplings g, g' , together with $\tan \beta = 1$ and $m_A = 0$ [26]). Subsequently, the presence (at the tree-level) of more than these two free parameters in the Higgs sector would be associated to the hard breaking of supersymmetry. The most general parameterization of such a breaking leading back to the general THDM discussed in the previous section, can be cast in the form:

$$\begin{aligned} \lambda_1 = \lambda_2 + \delta_{12} \quad , \quad \lambda_3 = \frac{1}{8}(g^2 + g'^2) - \lambda_1 + \delta_{31} \\ \lambda_4 = 2\lambda_1 - \frac{1}{2}g'^2 + \delta_{41} \quad , \quad \lambda_5 = -\frac{1}{2}(g^2 + g'^2) + 2\lambda_1 + \delta_{51} \\ \lambda_6 = -\frac{1}{2}(g^2 + g'^2) + 2\lambda_1 + \delta_{61} \end{aligned} \quad (15)$$

²quantum corrections should be consistently omitted here, as they contribute non-leading effects to the one-loop corrected $e^+e^- \rightarrow H^+H^-$, see also discussion in section 5

where the δ 's measure the amount of hard breaking of supersymmetry.

The various Higgs masses and $\tan 2\alpha$ can then be related to the δ 's upon use of the above equations in conjunction with eq.(2-4) as,

$$\begin{aligned} \tan 2\alpha &= \tan 2\beta \frac{m_A^2 + m_Z^2 - v^2(\delta_{51} + \delta_{61} + 4\delta_{31})}{m_A^2 - m_Z^2 - v^2(-\delta_{51} + \delta_{61} + 4\delta_{31} + 4\frac{\tan^2\beta}{1-\tan^2\beta}\delta_{12})} \\ m_{H^\pm}^2 &= m_A^2 + m_W^2 + v^2(\delta_{41} - \delta_{61}) \\ m_H^2 + m_h^2 &= m_A^2 + m_Z^2 + v^2(4\delta_{31} + \delta_{51} - \delta_{61} - 4\sin^2\beta\delta_{12}) \\ m_H^2 - m_h^2 &= \sqrt{(\cos 2\beta(m_Z^2 - m_A^2 + v^2(-\delta_{51} + \delta_{61} + 4\delta_{31} + 4\frac{\tan^2\beta}{1-\tan^2\beta}\delta_{12})))^2(1 + \tan^2 2\alpha)} \end{aligned} \quad (16)$$

Now the crucial point is to note that the MSSM tree-level mass-sum-rules,

$$m_{H^0, h^0}^2 = \frac{1}{2}(m_Z^2 + m_A^2 \pm \sqrt{(m_Z^2 + m_A^2)^2 - 4m_Z^2 m_A^2 \cos^2 2\beta}) \quad (17)$$

$$m_{H^\pm}^2 = m_A^2 + m_W^2 \quad (18)$$

as well as

$$\tan 2\alpha = \tan 2\beta \frac{m_A^2 + m_Z^2}{m_A^2 - m_Z^2} \quad (19)$$

can be recovered *not only in the susy case $\delta's = 0$, but actually in a full one-parameter subspace*. Indeed the validity of eq.(17-19) requires the following equations

$$\begin{aligned} \delta_{51} + \delta_{61} + 4\delta_{31} &= 0 \quad , \quad \delta_{61} - \delta_{51} + 4\delta_{31} + 4\frac{\tan^2\beta}{1-\tan^2\beta}\delta_{12} = 0 \\ \delta_{41} - \delta_{61} &= 0 \quad , \quad 4\delta_{31} + \delta_{51} - \delta_{61} - 4\sin^2\beta\delta_{12} = 0 \end{aligned} \quad (20)$$

which are satisfied if

$$\begin{aligned} \delta_{12} &= \frac{(\tan^4\beta - 1)}{\tan^4\beta}\delta_{31} \quad , \quad \delta_{51} = \frac{-2(1 + \tan^2\beta)}{\tan^2\beta}\delta_{31} \\ \delta_{61} = \delta_{41} &= \frac{2(1 - \tan^2\beta)}{\tan^2\beta}\delta_{31} \end{aligned} \quad (21)$$

With the above four constraints, we have just one extra free parameter as compared to the MSSM case, ex. δ_{31} or equivalently λ_3 eq.(15) on top of m_A and $\tan\beta$. Eqs.(21) together with the set of free parameters $(\lambda_3, m_A, \tan\beta)$, define our quasi-susy (QSUSY) parameterization. Obviously, when λ_3 hits its supersymmetric value, i.e. when $\delta_{31} = 0$, we get back the MSSM case, otherwise $\Delta\lambda_3 = \lambda_3 - \lambda_3^{susy}$ can be seen as measuring the ‘‘hardness’’ of the susy breaking, while m_A and $\tan\beta$ play the same role as in the MSSM.

There is a subtlety, however, as concerns the sign of $\sin 2\alpha$. Eqs.(21) are sufficient to lead to a looser constraint as compared to the well-known supersymmetric constraint [28] $\sin 2\alpha < 0$. Actually one can show that³

³ Detailed derivation of these and subsequent results related to QSUSY parameterization in the full Higgs sector including the leading one-loop corrections, will be given elsewhere

- a) $\sin 2\alpha < 0$ can be chosen in all the parameter space;
- b) $\sin 2\alpha > 0$ is possible provided $\cos 2\alpha < 0$, $\tan \beta < 1$ and $m_A < m_Z$;

Case b) means that the only consistent choice becomes $\sin 2\alpha < 0$ as soon as $\tan \beta > 1$ or $m_A > m_Z$. Since in our study we assume a very heavy charged Higgs ($m_{H^\pm} > 2m_Z$), thus a very heavy CP-odd neutral Higgs, eq.(18), we will stick to the choice $\sin 2\alpha < 0$ throughout the paper. One can then determine uniquely the behavior of the various couplings in terms of $\lambda_3, m_A, \tan \beta$:

$$\begin{aligned} g_{H^0 H^+ H^-} &= g_{H^0 H^+ H^-}^{MSSM} - igm_W \left(\frac{1}{2c_w^2} + \frac{m_A^2}{m_W^2} + \frac{s_w^2}{\pi\alpha} \lambda_3 \right) \tan \beta \\ g_{h^0 H^+ H^-} &= g_{h^0 H^+ H^-}^{MSSM} - igm_W \frac{2m_A^2}{m_A^2 - m_Z^2} \left(\frac{1}{2c_w^2} + \frac{m_A^2}{m_W^2} + \frac{s_w^2}{\pi\alpha} \lambda_3 \right) \end{aligned} \quad (22)$$

where

$$\begin{aligned} g_{H^0 H^+ H^-}^{MSSM} &= -ig(m_W \cos(\beta - \alpha) - \frac{m_Z}{2c_w} \cos 2\beta \cos(\beta + \alpha)) \\ g_{h^0 H^+ H^-}^{MSSM} &= -ig(m_W \sin(\beta - \alpha) + \frac{m_Z}{2c_w} \cos 2\beta \sin(\beta + \alpha)) \\ g_{H^0 H^\pm G^\mp} &= \frac{-ig \sin(\beta - \alpha)(m_{H^\pm}^2 - m_H^2)}{2m_W} \\ g_{h^0 H^\pm G^\mp} &= \frac{ig \cos(\beta - \alpha)(m_{H^\pm}^2 - m_h^2)}{2m_W} \\ g_{A^0 H^\pm G^\mp} &= \mp \frac{m_{H^\pm}^2 - m_A^2}{2m_W} \end{aligned} \quad (23)$$

2.3 Charged Higgs-bosons interactions with gauge-bosons

The Higgs-bosons interactions with gauge-bosons are model independent. These interactions arise from the covariant derivatives in the Lagrangian:

$$\sum_i (D_\mu \Phi_i)^\dagger (D_\mu \Phi_i) = \sum_i [(\partial_\mu + ig\vec{T}_a W_\mu^a + ig' \frac{Y_{\Phi_i}}{2} B_\mu) \Phi_i]^\dagger (\partial_\mu + ig\vec{T}_a W_\mu^a + ig' \frac{Y_{\Phi_i}}{2} B_\mu) \Phi_i \quad (24)$$

where: \vec{T}_a are the isospin gauge generators, Y_{Φ_i} the hypercharge of the Higgs fields, W_μ^a the $SU(2)_L$ gauge fields, B_μ the $U(1)_Y$ gauge field, and g (resp. g') the associated coupling constants.

From eq. (24), one can easily extract the coupling of charged Higgs pair to the photon A_μ , and Z boson Z_μ . The corresponding Feynman rules read,

$$A_\mu H^+ H^- = -ie(k_1 - k_2)_\mu \quad , \quad Z_\mu H^+ H^- = -ie \frac{c_W^2 - s_W^2}{2s_W c_W} (k_1 - k_2)_\mu \quad (25)$$

Where $k_{1,2}$ are the incoming momentum of the charged Higgs boson. Note that these vertices depend only on standard parameters (the electric charge and Weinberg angle).

At tree-level, the $H^\pm W^\mp A_\mu$ vertex does not exist as a consequence of the conservation of the electromagnetic current. On the contrary the vanishing of the $H^\pm W^\mp Z_\mu$ vertex is accidental, (see [29] for further discussions). A consequence of the absence of these two vertices at tree-level is that the mixing $H^\pm - W^\mp$ is not present in our study. From eq. (24) we can get also all the Feynman rules for the three and four point vertices involving Higgs and gauge bosons. Obviously all these Feynman rules have of the same structure in any THDM, irrespective of the implementation of supersymmetry, and depend only on the mixing angles α and β (Appendix C). The only impact of SUSY there, as compared to a general THDM model, would be to require $\sin 2\alpha \leq 0$.

2.4 Charged Higgs-bosons interactions with fermions

In the two Higgs doublets extension of the standard model, there exist two different ways to couple Higgs fields to matter: either **type I** where the quarks and leptons couple exclusively to one of the two Higgs doublets, exactly as in the minimal standard model and will not be considered further in this paper, or the **type II** where, to avoid the problem of Flavor Changing Neutral Current (FCNC) [30], Φ_1 couples only to down quarks (and charged leptons) and Φ_2 couples only to up quarks (and neutral leptons). This latter model is the pattern found in the MSSM. In this case, the charged Higgs interaction to fermions is given by:

$$H^- u \bar{d} = \frac{g V_{ud}}{\sqrt{2} m_W} \left(Y_u \frac{(1 - \gamma_5)}{2} + Y_d \frac{(1 + \gamma_5)}{2} \right) \quad (26)$$

where $Y_u = \frac{m_u}{\tan \beta}$ and $Y_d = \tan \beta m_d$, V_{ud} is the Kobayashi–Maskawa matrix element which we will take close to one.

3 Notations, conventions and cross section in the lowest order.

In this paper we will use the following notations and conventions. The momentum of the outgoing electron and positron and incoming Higgs bosons H^+ , H^- are denoted by p_1 , p_2 , k_1 and k_2 , respectively. Neglecting the electron mass m_e (and also the electron–Higgs couplings which is proportional to m_e), the momenta in the center-of-mass system of the $e^+ e^-$ are given by:

$$p_{1,2} = \frac{\sqrt{s}}{2} (1, 0, 0, \pm 1)$$

$$k_{1,2} = \frac{\sqrt{s}}{2} (1, \pm \kappa \sin \theta, 0, \pm \kappa \cos \theta)$$

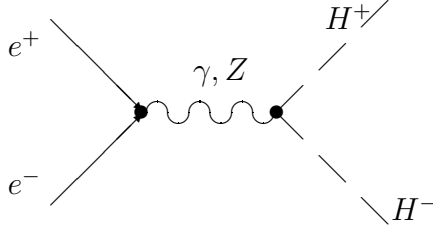
where $\sqrt{s}/2$ denotes the beam energy, θ the scattering angle between the e^+ and H^+ flight directions in the laboratory frame, $\kappa^2 = 1 - \frac{4m_{H^\pm}^2}{s}$, and m_{H^\pm} the mass of the charged

Higgs.

The Mandelstam variables are defined as follow:

$$\begin{aligned}
s &= (p_1 + p_2)^2 = (k_1 + k_2)^2 \\
t &= (p_1 - k_1)^2 = (p_2 - k_2)^2 = m_{H^+}^2 - \frac{s}{2} + \frac{s}{2}\kappa \cos \theta \\
u &= (p_1 - k_2)^2 = (p_2 - k_1)^2 = m_{H^+}^2 - \frac{s}{2} - \frac{s}{2}\kappa \cos \theta \\
s + t + u &= 2m_{H^+}^2
\end{aligned}$$

The only Feynman diagrams contributing at the tree-level are the γ and Z s-channel exchange, [the electron-Higgs coupling being negligibly small, there is no t-channel contribution at this order.]



The contributions to the lowest-order amplitude have the following form:

$$\mathcal{M}_0^\gamma = -2 \frac{e^2}{s} \bar{v}(p_2) \not{k}_1 u(p_1) \quad (27)$$

$$\mathcal{M}_0^Z = 2 \frac{e^2 g_H}{s - m_z^2} (g_V \bar{v}(p_2) \not{k}_1 u(p_1) - g_A \bar{v}(p_2) \not{k}_1 \gamma^5 u(p_1)) \quad (28)$$

where $g_V = (1 - 4s_W^2)/(4c_W s_W)$, $g_A = 1/(4c_W s_W)$, $g_H = -(c_W^2 - s_W^2)/(2c_W s_W)$, $c_W \equiv \cos \theta_W$, $s_W \equiv \sin \theta_W$.

As one can see from eq. (27, 28), those amplitudes can be expressed in terms of two invariants, I_V and I_A defined as:

$$I_V = \bar{v}(p_2) \not{k}_1 u(p_1), \quad I_A = \bar{v}(p_2) \not{k}_1 \gamma^5 u(p_1) \quad (29)$$

The Born amplitude is given by:

$$\mathcal{M}_0 = \mathcal{M}_0^\gamma + \mathcal{M}_0^Z \quad (30)$$

From eqs. (27, 28), the corresponding differential cross section first studied in [21] is found to be,

$$\left(\frac{d\sigma}{d\Omega} \right)_0 = \frac{\alpha^2 \kappa^3}{8s} \left(1 + g_H^2 \frac{g_V^2 + g_A^2}{(1 - m_Z^2/s)^2} - \frac{2g_H g_V}{1 - m_Z^2/s} \right) \sin^2 \theta \quad (31)$$

The total cross-section is:

$$\sigma_{tot} = \frac{\pi\alpha^2\kappa^3}{3s} \left(1 + g_H^2 \frac{g_V^2 + g_A^2}{(1 - m_Z^2/s)^2} - \frac{2g_H g_V}{1 - m_Z^2/s} \right) \quad (32)$$

At this stage we note the characteristic angular distribution of spin zero scalar particles which is expressed as:

$$\frac{2\pi}{\sigma_{tot}} \left(\frac{d\sigma}{d\Omega} \right)_0 = \frac{3}{4} \sin^2 \theta$$

This angular dependence leads to a vanishing forward–backward asymmetry A_{FB} at tree-level, where

$$A_{FB} = \frac{\int_{\theta \leq \pi/2} d\Omega \frac{d\sigma}{d\Omega} - \int_{\theta \geq \pi/2} d\Omega \frac{d\sigma}{d\Omega}}{\int_{\theta \leq \pi/2} d\Omega \frac{d\sigma}{d\Omega} + \int_{\theta \geq \pi/2} d\Omega \frac{d\sigma}{d\Omega}}$$

As we will see in the next section, at the one-loop level, only box diagrams can give contributions to A_{FB} .

4 Radiative corrections.

We have evaluated the radiative corrections at the one-loop level in the 't Hooft–Feynman gauge. These one-loop corrections are ultraviolet (UV) and infrared (IR) divergent. The UV singularities are treated by dimensional regularization in the on–mass–shell renormalization scheme while the IR singularities are regularized with a small fictitious photon mass m_γ . We renormalize not only the masses and coupling constants, but also the field wave functions in such a way that the residues of renormalized propagators are equal to one.

The typical Feynman diagrams for the virtual corrections of order α^2 are drawn in figure 1. These comprise, the THDM contribution to the photon and Z propagator and their mixing (Fig.1.1), the standard contribution to the initial state (Fig. 1.2, 1.3 and 1.4), the THDM contribution to the final vertex (Fig. 1.5–1.12) and the THDM box contributions (Fig. 1.13 and 1.14). The amplitudes of the Feynman diagrams depicted in Fig. 1.15 and Fig. 1.16 are proportional to the electron mass and thus negligible. Bremsstrahlung diagrams and diagrams with a virtual photon emission are shown in Fig 1.17–1.28. Diagrams 1.29–1.33 are needed for charged Higgs wave function renormalization.

Note that one loop contributions coming from initial state $e^+e^-H_0$ and $e^+e^-h_0$ vertices are also vanishing like m_e , since e^+ and e^- are both on-shell. A similar argument holds for the A^0 and neutral goldstone exchange diagrams, as well as $Z - A^0$ and $Z - G^0$ mixing, noting also that $A^0 H^+ H^-$ and $G^0 H^+ H^-$ couplings are already forbidden at tree-level by CP invariance.

Those Feynman diagrams are generated and computed using FeynArts and FeynCalc packages [31] supplied with a full MSSM and THDM-II Feynman rules code [32]. We also used the Fortran FF-package [33], in the numerical analysis. The one loop amplitude \mathcal{M}^1 projects fully on the two invariants defined in eq.(29) as

$$\mathcal{M}^1 = \mathcal{M}_A^1 I_A + \mathcal{M}_V^1 I_V \quad (33)$$

The typical one loop contributions are given in this form in terms of the Passarino–Veltman functions in appendix C and D.

The diagrams of figure 1: 1.22 and 1.25–1.28 together with real Bremsstrahlung 1.17–1.20 are needed to yield an IR finite corrected differential cross section (1.21, 1.23, 1.24 are free from IR divergencies) which has the following form:

$$\left(\frac{d\sigma}{d\Omega}\right)_1 = \left(\frac{d\sigma}{d\Omega}\right)_0 + \left(\frac{d\sigma}{d\Omega}\right)_{SB} + 2Re(\mathcal{M}_0^* \mathcal{M}^1) \frac{\kappa}{64\pi^2 s} \quad (34)$$

Here $\left(\frac{d\sigma}{d\Omega}\right)_{SB}$ denotes the soft Bremsstrahlung contribution. Using eqs. (27–30 and 33) the term $Re(\mathcal{M}_0^* \mathcal{M}^1)$ reads:

$$Re(\mathcal{M}_0^* \mathcal{M}^1) = [\mathcal{M}_A^1 \left(-\frac{e^2 g_H g_A}{4(s - m_Z^2)} s^2 \kappa^2 \right) + \mathcal{M}_V^1 \left(\frac{e^2}{4} \kappa^2 (-s + s^2 \frac{g_H g_V}{(s - m_Z^2)}) \right)] \sin^2 \theta \quad (35)$$

As one can see from the last formula the interference term is proportional to $\sin^2 \theta$. Consequently, since vertex and self-energy contributions to $\mathcal{M}_{A,V}^1$ have only s dependence, they will not contribute to the forward-backward asymmetry A_{FB} . Only box diagrams can contribute to A_{FB} through their t and u dependence.

Let us cast the various one-loop corrections in the form:

$$\sigma_1 = \sigma_0(1 + \delta) = \sigma_0(1 + \delta_{soft}^\gamma + \delta_{fermions} + \delta_{bosons}) \quad (36)$$

where δ_{soft}^γ is the full (IR finite) set of one-loop QED contributions of diagrams 1.22–1.28 and of 1.17–1.21 with soft photon emission of figure 1, $\delta_{fermions}$ is the full vertex and self-energy contributions of all leptons and quarks, δ_{bosons} the massive gauge boson and Higgs contributions in vertices self-energies and boxes.

4.1 On-mass-shell Renormalization.

The parameters entering the tree-level observables eqs.(31–32) are all standard model parameters, except for the charged Higgs mass itself. This fact will render the one-loop renormalization rather simple, in the sense that all non-standard parameters appearing first at the one-loop level, will not get renormalized. In particular, renormalization conditions related to the definition of $\tan \beta$ are not explicitly needed here. We will need, however, to renormalize the charged Higgs wave-function and mass. On the other hand, the renormalization scheme should be chosen in such a way to allow a simple interpolation between the MSSM and the THDM-II. If we choose to renormalize m_{A^0} on-shell, identifying the pole of the propagator with the mass parameter in the renormalized Lagrangian \mathcal{L}_R , then m_{H^\pm} would be uniquely determined in the MSSM, through the mass sum-rules, and its renormalized quantity would be shifted from the corresponding mass parameter in \mathcal{L}_R , [8]. In the THDM-II case, one would then need to define, somewhat artificially, the renormalized m_{H^\pm} also to depart from the corresponding parameter in \mathcal{L}_R , though in such a way that one recovers the MSSM situation when $\lambda_i \rightarrow \lambda_i^{MSSM}$. To avoid such

complications, the simplest will be to take in the MSSM m_{H^\pm} as a free parameter (rather than m_{A^0}) and renormalize it on-shell. This allows to treat the MSSM and THDM-II cases at equal footing in the charged Higgs sector, with a unique renormalization scheme.

We will adopt throughout, the renormalization scheme of refs. [34]–[35]. In this scheme one renormalizes all the fields before electroweak symmetry breaking. A renormalization constant $Z_{\Phi_{1,2}}$ is introduced for each doublet $\Phi_{1,2}$, Z_2^W for the $SU_L(2)$ triplet W_μ^a and Z_2^B for the $U(1)$ singlet. The gauge fields, coupling constants and vacuum expectation values v_i are renormalized as follow:

$$\begin{aligned} W_\mu^a &\rightarrow (Z_2^W)^{1/2} W_\mu^a \\ B_\mu &\rightarrow (Z_2^B)^{1/2} B_\mu \\ \Phi_i &\rightarrow (Z_{\Phi_i})^{1/2} \Phi_i \\ g &\rightarrow (Z_1^W)(Z_2^W)^{-3/2} g \\ g' &\rightarrow (Z_1^B)(Z_2^B)^{-3/2} g' \\ v_i &\rightarrow (Z_{\Phi_i})^{1/2} (v_i - \delta v_i) \end{aligned} \tag{37}$$

In the on-mass-shell scheme the counterterms can be fixed by the following renormalization conditions:

- The on-shell conditions for m_W , m_Z , m_e and the electric charge e are defined as in the standard model [34].
- On-shell condition for the charged Higgs boson H^\pm : we choose to identify the physical charged Higgs mass with the corresponding parameter in $\mathcal{L}_\mathcal{R}$, and require the residue of the propagator to have its tree-level value, i.e.,

$$\delta m_{H^\pm}^2 = \text{Re} \sum^{H^+ H^+} (m_{H^\pm}^2) \quad \text{and} \quad \delta Z^{H^\pm} = \frac{\partial}{\partial p^2} (\sum^{H^+ H^+} (p^2))|_{p^2=m_{H^\pm}^2} \tag{38}$$

where $\sum^{H^+ H^+} (p^2)$ is the charged Higgs bare self-energy.

- Tadpoles are renormalized in such a way that the renormalized tadpoles vanish: $T_h + \delta t_h = 0$, $T_H + \delta t_H = 0$. These conditions guarantee that $v_{1,2}$ appearing in $\mathcal{L}_\mathcal{R}$ are located at the minimum of the one-loop potential.

As we are looking for a charged Higgs bosons pair production and using m_{H^\pm} and $\tan\beta$ as independent parameters (in the Higgs sector), we can choose a renormalization scheme very close to that of [35]. The main difference with [35] being that we renormalize the charged Higgs on-shell rather than the CP-odd A_0 .

To compute the counterterms necessary to our study, we have to make all the substitutions given in eqs.(37) in the covariant derivative and replace the renormalization constants Z_i by their expansion up to first order, $Z_i = 1 + \delta Z_i$. Those transformations shift $(D_\mu \Phi_i)^+ (D_\mu \Phi_i)$ to the corresponding expression in terms of renormalized fields and

couplings plus a set of counterterms. In our case we need just the two following ones:

$$\begin{aligned}\delta(A_\mu H^+ H^-) &= -ie[\delta Z^{H^\pm} + (\delta Z_1^\gamma - \delta Z_2^\gamma) + g_H(\delta Z_1^{\gamma Z} - \delta Z_2^{\gamma Z})](k_1 - k_2)_\mu \\ \delta(Z_\mu H^+ H^-) &= ie g_H[\delta Z^{H^\pm} + (\delta Z_1^Z - \delta Z_2^Z) + \frac{1}{g_H}(\delta Z_1^{\gamma Z} - \delta Z_2^{\gamma Z})](k_1 - k_2)_\mu\end{aligned}\quad (39)$$

where δZ^{H^\pm} is related to $\delta Z_{\Phi_{1,2}}$ by the relation $\delta Z^{H^\pm} = \sin^2 \beta \delta Z_{\Phi_1} + \cos^2 \beta \delta Z_{\Phi_2}$, the δZ_i^γ , δZ_i^Z and $\delta Z_i^{\gamma Z}$ are related to δZ_i^W and δZ_i^B as in [35]⁴.

$$\begin{aligned}\delta Z_i^\gamma &= s_W^2 \delta Z_i^W + c_W^2 \delta Z_i^B \\ \delta Z_i^Z &= c_W^2 \delta Z_i^W + s_W^2 \delta Z_i^B \\ \delta Z_i^{\gamma Z} &= -c_W s_W (\delta Z_i^W - \delta Z_i^B) = \frac{-c_W s_W}{c_W^2 - s_W^2} (\delta Z_i^Z - \delta Z_i^\gamma)\end{aligned}$$

Moreover, in the on-shell scheme defined in ref [34], the wave function renormalization constants of the gauge bosons are given by:

$$\delta Z_2^\gamma = -\frac{\partial \Sigma^\gamma}{\partial p^2}(0) \quad (40)$$

$$\delta Z_1^\gamma = \delta Z_2^\gamma + \frac{s_W}{c_W} \frac{\Sigma^{\gamma Z}(0)}{m_Z^2} \quad (41)$$

$$\delta Z_2^Z = \delta Z_2^\gamma + 2 \frac{c_W^2 - s_W^2}{s_W c_W} \frac{\Sigma^{\gamma Z}(0)}{m_Z^2} + \frac{c_W^2 - s_W^2}{s_W^2} \left(\frac{\delta m_Z^2}{m_Z^2} - \frac{\delta m_W^2}{m_W^2} \right) \quad (42)$$

$$\delta Z_1^Z = \delta Z_2^Z + \frac{3c_W^2 - 2s_W^2}{s_W c_W} \frac{\Sigma^{\gamma Z}(0)}{m_Z^2} + \frac{c_W^2 - s_W^2}{s_W^2} \left(\frac{\delta m_Z^2}{m_Z^2} - \frac{\delta m_W^2}{m_W^2} \right) \quad (43)$$

$$\delta Z_{1,2}^{\gamma Z} = -\frac{c_W s_W}{c_W^2 - s_W^2} (\delta Z_{1,2}^Z - \delta Z_{1,2}^\gamma) \quad (44)$$

Using these relations, one finds for the renormalization constants appearing in eq. (39):

$$\delta Z_1^\gamma - \delta Z_2^\gamma = \frac{s_W}{c_W} \frac{\Sigma^{\gamma Z}(0)}{m_Z^2} = -\frac{\alpha}{2} B_0(0, m_W^2, m_W^2) \quad (45)$$

$$\delta Z_1^Z - \delta Z_2^Z = \frac{c_W}{s_W} \frac{\Sigma^{\gamma Z}(0)}{m_Z^2} = -\frac{\alpha c_W^2}{2s_W^2} B_0(0, m_W^2, m_W^2) \quad (46)$$

$$\delta Z_1^{\gamma Z} - \delta Z_2^{\gamma Z} = -\frac{\Sigma^{\gamma Z}(0)}{m_Z^2} = \frac{\alpha c_W}{2s_W} B_0(0, m_W^2, m_W^2) \quad (47)$$

Note that the above combinations are independent of the fermion and charged Higgs contributions because $\Sigma^{\gamma Z}(p^2)$ is vanishing at $p^2 = 0$.

The renormalization constant of the charged Higgs wave function is given by:

$$\delta Z^{H^\pm} = \delta Z_{bosons}^{H^\pm} + \delta Z_{fermions}^{H^\pm} \quad (48)$$

⁴note ,however, a difference in the convention for the sign of the Weinberg angle θ_W .

with:

$$\begin{aligned}
\delta Z_{bosons}^{H^\pm} = & \frac{\alpha}{4\pi s_W^2} (2s_W^2 (B_0(m_{H^\pm}^2, 0, m_{H^\pm}^2) + 2m_{H^\pm}^2 B'_0(m_{H^\pm}^2, m_\gamma^2, m_{H^\pm}^2)) + \\
& \frac{1}{2} B_0(m_{H^\pm}^2, m_A^2, m_W^2) + \frac{c_{\beta\alpha}^2}{2} B_0(m_{H^\pm}^2, m_h^2, m_W^2) + \frac{s_{\beta\alpha}^2}{2} B_0(m_{H^\pm}^2, m_H^2, m_W^2) + \\
& \frac{(-1 + 2s_W^2)^2}{2c_W^2} B_0(m_{H^\pm}^2, m_{H^\pm}^2, m_Z^2) - g_{hH^+H^-}^2 B'_0(m_{H^\pm}^2, m_h^2, m_W^2) + \\
& \frac{1}{4} (2m_A^2 + 2m_{H^\pm}^2 - m_W^2 - 4g_{AH^+G^-}^2 s_W^2) B'_0(m_{H^\pm}^2, m_A^2, m_W^2) \\
& + \frac{1}{4} (c_{\beta\alpha}^2 (2m_h^2 + 2m_{H^\pm}^2 - m_W^2) - 4g_{hH^+G^-}^2 s_W^2) B'_0(m_{H^\pm}^2, m_h^2, m_W^2) \\
& - g_{HH^+H^-}^2 B'_0(m_{H^\pm}^2, m_H^2, m_W^2) + \frac{1}{4} (s_{\beta\alpha}^2 (2m_H^2 + 2m_{H^\pm}^2 - m_W^2) \\
& - 4g_{HH^+G^-}^2 s_W^2) B'_0(m_{H^\pm}^2, m_H^2, m_W^2) + \frac{(4m_{H^\pm}^2 - m_Z^2)}{4c_W^2} (c_W^2 - s_W^2)^2 B'_0(m_{H^\pm}^2, m_{H^\pm}^2, m_Z^2)) \\
\delta Z_{fermions}^{H^\pm} = & \frac{N_C \alpha}{8\pi m_W^2 s_W^2} (-(Y_u^2 + Y_d^2) B_0(m_{H^\pm}^2, m_d^2, m_u^2) \\
& + ((m_d^2 + m_u^2 - m_{H^\pm}^2)(Y_u^2 + Y_d^2) + 4m_d m_u Y_u Y_d) B'_0(m_{H^\pm}^2, m_d^2, m_u^2))
\end{aligned} \tag{49}$$

where $\{c, s\}_{\beta\alpha} = \{\cos, \sin\}(\beta - \alpha)$, Y_u and Y_d are defined in eq. (26). $N_C = 3$ for quarks and 1 for leptons. The couplings $g_{AH^+G^-}$, $g_{hH^+H^-}$, $g_{HH^+H^-}$, $g_{hH^+G^-}$ and $g_{HH^+G^-}$ are trilinear scalar couplings which are model dependent. B'_0 is the derivative of the B_0 function with respect to the square of the charged Higgs 4-momentum taken at $p_{H^\pm}^2 = m_{H^\pm}^2$. In the above expressions, only $B'_0(m_{H^\pm}^2, m_\gamma^2, m_{H^\pm}^2)$ contains infrared divergences, regulated here by m_γ which should cancel with the appropriate Bremsstrahlung contributions.

To sum up, most divergences (including initial state $\gamma e^+ e^-$ and $Ze^+ e^-$ vertices, and Z and γ self-energies and mixing) are absorbed in the renormalization of the standard parameters, the electric charge, M_Z , M_W , m_e and the wave functions, as usual. The one-loop correction to the H^\pm self-energy cancels out when the Higgs pair is produced on shell. The only remaining non-standard renormalization is that of $\gamma H^+ H^-$ and $Z H^+ H^-$ vertices, given by eqs. (39). Furthermore, its model-dependence is exclusively contained in the charged Higgs wave function renormalization constant δZ^{H^\pm} as can be seen from eqs. (48, 49). Hence the renormalization procedure will involve essentially a set of (standard) parameters, which, combined with the quasi-susy parameterization of section 2, would facilitate a simultaneous treatment and comparison of THDM-II and MSSM cases.

4.2 Bremsstrahlung

In order to have an IR finite result we have to add to the cross section the contribution from $e^+ e^- \rightarrow H^+ H^- \gamma$ in the soft-photon limit; the relevant diagrams are drawn in Fig. 1.17-1.28.

Denoting the photon four-momentum by k and its polarization vector by $\epsilon_\mu(k)$ the

amplitude of the soft Bremsstrahlung can be written in the form,

$$\begin{aligned}\epsilon_\mu \mathcal{M}_{SB}^\mu &= e \mathcal{M}_{Born} \left(\frac{p_1 \epsilon}{p_1 k} - \frac{p_2 \epsilon}{p_2 k} + \frac{k_2 \epsilon}{k_2 k} - \frac{k_1 \epsilon}{k_1 k} \right) \\ &\quad - 2e^3 \bar{v}(p_2) \not{\epsilon} \left(\frac{1}{s} + \frac{g_H(-g_V + g_A \gamma^5)}{s - m_z^2} \right) u(p_1).\end{aligned}\quad (50)$$

The differential cross section is as follows:

$$\begin{aligned}\left(\frac{d\sigma}{d\Omega} \right)_{SB} &= \left(\frac{d\sigma}{d\Omega} \right)_0 \delta_{SB} \\ &+ 8 \frac{\alpha^3}{s} \left(1 - \frac{2g_V g_H}{1 - m_Z^2/s} + \frac{g_H^2(g_V^2 + g_A^2)}{(1 - m_Z^2/s)^2} \right) (I_0 - \frac{s}{4} \kappa^2 \sin^2 \theta (I_1 + I_2))\end{aligned}\quad (51)$$

where δ_{SB} , I_0 , I_1 and I_2 are given by,

$$\begin{aligned}\delta_{SB} &= -\frac{\alpha}{\pi} \left\{ 2 \ln \left(\frac{4\Delta E^2}{m_\gamma^2} \right) - \ln \left(\frac{4\Delta E^2}{m_\gamma^2} \right) \ln \left(\frac{s}{m_e^2} \right) + \ln \left(\frac{m_e^2}{s} \right) + \frac{1}{\kappa} \ln \left(\frac{1-\kappa}{1+\kappa} \right) \right. \\ &\quad + \frac{1+\kappa^2}{2\kappa} \ln \left(\frac{4\Delta E^2}{m_\gamma^2} \right) \ln \left(\frac{1-\kappa}{1+\kappa} \right) + 2 \ln \left(\frac{4\Delta E^2}{m_\gamma^2} \right) \ln \left(\frac{m_{H^+}^2 - u}{m_{H^+}^2 - t} \right) \\ &\quad + \frac{\pi^2}{3} + \frac{1}{2} \ln^2 \left(\frac{m_e^2}{s} \right) + \frac{1+\kappa^2}{\kappa} \left[Li_2 \left(\frac{2\kappa}{1+\kappa} \right) + \frac{1}{4} \ln^2 \left(\frac{1-\kappa}{1+\kappa} \right) \right] \\ &\quad + 2 \left[Li_2 \left(1 - \frac{s(1-\kappa)}{2(m_{H^+}^2 - t)} \right) + Li_2 \left(1 - \frac{s(1+\kappa)}{2(m_{H^+}^2 - t)} \right) \right. \\ &\quad \left. \left. - Li_2 \left(1 - \frac{s(1-\kappa)}{2(m_{H^+}^2 - u)} \right) - Li_2 \left(1 - \frac{s(1+\kappa)}{2(m_{H^+}^2 - u)} \right) \right] \right\}\end{aligned}\quad (52)$$

$$I_0 = \kappa \left(\frac{\Delta E^2}{2} + \frac{\Delta E}{2\sqrt{s}} m_{H^\pm}^2 \right) + \frac{m_{H^\pm}^2}{2} \left(1 - \frac{m_{H^\pm}^2}{s} \right) \ln \left(\frac{(1-\kappa)^2}{(1-\kappa)^2 + 4\frac{\Delta E}{\sqrt{s}} \kappa} \right)$$

$$I_1 = I_2 = (1 + \kappa^2) \ln \left(\frac{(1-\kappa)^2}{(1-\kappa)^2 + 4\frac{\Delta E}{\sqrt{s}} \kappa} \right)\quad (53)$$

after integration over the photon momentum subject to $|\vec{k}| < \Delta E$, ΔE defining the soft photon energy cut-off for the Bremsstrahlung process. The infrared divergence is regulated by a fictitious small photon mass m_γ .

We have checked algebraically and numerically that m_γ cancels out when the Bremsstrahlung cross-section is added to the rest. Note also that the Sudakov effects $\ln^2(m_e^2/s)$ cancel with the QED diagrams in the initial state. Numerically, we find that the second term of the right-hand side of eq. (51) is very small compared to the term proportional to δ_{SB} and can

be ignored.

Note finally that we assume throughout the study that hard bremsstrahlung is suitably separated. This relies of course on the quality of the veto on real photons in the final state.

5 Numerical analysis and discussion.

The following experimental input are taken for the physical parameters [36]:

- the fine structure constant, $\alpha = \frac{e^2}{4\pi} = 1/137.03598$.
- the gauge boson masses, $m_Z = 91.187 \text{ GeV}$, $m_W = 80.41 \text{ GeV}$.
- the input lepton masses:

$$m_e = 0.511 \text{ MeV} \qquad m_\mu = 0.1057 \text{ GeV} \qquad m_\tau = 1.784 \text{ GeV}$$

- for the light quark masses we use the effective values which are chosen in such a way that the experimentally extracted hadronic part of the vacuum polarizations is reproduced [37]:

$$\begin{array}{lll} m_d = 46 \text{ MeV} & m_u = 46 \text{ MeV} & m_s = 150 \text{ MeV} \\ m_c = 1.5 \text{ GeV} & m_b = 4.5 \text{ GeV} & \end{array}$$

The top quark mass is taken to be 175 GeV. In the on-shell scheme we consider, $\sin^2 \theta_W$ is given by $\sin^2 \theta_W \equiv 1 - \frac{m_W^2}{m_Z^2}$ valid beyond tree-level. The derived value $\sin^2 \theta_W \simeq 0.23$ thus includes radiative corrections.

Fig.2 shows the integrated tree level cross section $\sigma_0(fb)$ as a function of charged Higgs mass for three values of \sqrt{s} . It can be seen that for a charged Higgs mass around 220–230 GeV and for an integrated luminosity of about 10 to 50 fb⁻¹ (for the corresponding energy of 500 GeV), a few hundred events of charged Higgs pairs are expected at LC2000. We can have the same situation for higher c.m. energies (1 TeV–2 TeV), for an integrated luminosity of about 200 fb⁻¹, and for charged Higgs mass not very close to its threshold value.

We now discuss separately the various contributions to the quantum corrections. We have listed in table 1 the contribution to the integrated cross section (in percent) and to the forward–backward asymmetry due to the soft–photon Bremsstrahlung and the virtual photon emission for several values of the soft–photon energy cut–off ΔE . The dependence on ΔE is rather important, for example, at $\sqrt{s} = 500 \text{ GeV}$ and for $m_{H^\pm} = 220 \text{ GeV}$ the correction increases from -10.8% for $\Delta E = 0.15E$ to reach -24.7% at $\Delta E = 0.05E$. The forward–backward asymmetry is small.

Note that contributions from the initial $e^+e^-\gamma$, (Z) vertices to the corrected cross section are typically standard and hence depend neither on $\tan \beta$ nor on the charged Higgs mass.

Those corrections are of order (without soft and virtual photon emission) 2.5% at $\sqrt{s} = 500$ GeV, 3.6% at $\sqrt{s} = 1000$ GeV and 4.3% at $\sqrt{s} = 1500$ GeV.

The standard boxes are not very sensitive to $\tan\beta$, but can give important contributions. For instance:

- at $\sqrt{s} = 500\text{GeV}$ the effect is about -9.5% for a Higgs mass of 110 GeV and -7.3% for a Higgs mass of 220 GeV.
- at $\sqrt{s} = 1000\text{GeV}$ the effect is about -13.3% for a Higgs mass of 230 GeV and -11.2% for a Higgs mass of 410 GeV.
- at $\sqrt{s} = 1500\text{GeV}$ the effect is about -15.9% for a Higgs mass of 410 GeV and -13.7% for a Higgs mass of 680 GeV.

We discuss now the contribution of fermions (light fermions and top-bottom) to the s-channel self-energy of the gauge bosons ($\gamma\text{--}\gamma$, $\gamma\text{--}Z$ and $Z\text{--}Z$) and to the $\gamma H^+ H^-$ and $Z H^+ H^-$ vertices. Light fermion contributions are positive and are not very sensitive to $\tan\beta$ and m_{H^\pm} . As can be seen from table 2, these contributions are substantial, around 16%–19%. The top-bottom contribution is very sensitive to $\tan\beta$ because of the form of the coupling given by eq.(26) which depends on the top-mass. One can see from eq.(26) that the top effect is enhanced either for small values of $\tan\beta$ through the top mass effect, or for very large values of $\tan\beta$ through the non vanishing bottom mass. In such regimes effects of the order of -25% can be reached, thus cancelling or even overwhelming the light fermion effects. Generically, however, the latter effects remain dominant for intermediate $\tan\beta$ values.

To discuss the contribution of the bosonic sector (Higgs bosons and gauge bosons contribution) to the the gauge boson self energy, the final state vertex and the box contributions⁵, we will use the QSUSY parameterization described in section II. This parameterization allows a comparison between the MSSM and THDM-II and is described only by three parameters m_{H^\pm} , $\tan\beta$ and λ_3 .

In Fig 3–5 we show the percentage contribution to the integrated cross section as a function of \sqrt{s} and for different values of λ_3 and $\tan\beta$. For $m_{H^\pm} = 220$ GeV one finds that when λ_3 takes its supersymmetric value λ_3^{MSSM} the bosonic contribution is about -10% at $\sqrt{s} \approx 500$ GeV (for both small and large $\tan\beta$) and increases with increasing c.m. energy, reaching -20 % to -25 % for $\sqrt{s} \approx 2\text{TeV}$. The correction is not very sensitive to the charged Higgs mass and interferes destructively with the fermionic contribution. In general, the bosonic contributions in the MSSM-like case tend to cancel the fermionic contributions for not too small (< 1) or not too large (~ 60) values of $\tan\beta$. When λ_3 is taken away from its supersymmetric value, the situation changes drastically. For a small deviation from λ_3^{MSSM} the effect is still of the same order as in the MSSM, but can get large and have both signs the farther we go from λ_3^{MSSM} , as can be seen from Fig.3,4,5. In some regions of the parameter space the effect can even grow too large for a reliable perturbative treatment, reaching more than 40% (!), without having enough cancellation (if any) from the

⁵Note that soft photon contributions have been subtracted and are given separately in table 1.

fermionic contribution. Such large effects can occur as a direct consequence of increasing $\tan\beta$, as illustrated in Fig. 6, but also for small $\tan\beta$ as illustrated in Fig. 4.a, 5.a when m_{H^\pm} is large enough (see eqs.(22)).

The total cross section $\sigma_1(fb)$ is plotted in figures 8 and 9 for two values of m_{H^\pm} and $\tan\beta$ and for various choices of λ_3 . Shown is the summed effect of all fermionic and bosonic contributions (initial state, final state vertex, self energies and non infrared boxes diagrams), excluding the gauge invariant set of diagrams containing at least one virtual photon exchange [the numerical contribution of the latter being mainly that of the IR sector]. When $\lambda_3 = \lambda_3^{MSSM}$ the net effect of radiative corrections remains small ($\lesssim 5\%$). In all cases we have illustrated, the one loop corrections generically decrease substantially the cross section for small $\tan\beta$ when λ_3 departs from λ_3^{MSSM} , while for large $\tan\beta$ the cross section can be increased in some cases.

Fig. 7 shows the one-loop forward-backward asymmetry A_{FB} as a function of \sqrt{s} . As one can see from this figure, A_{FB} is small; this is due to the fact that only box diagrams contribute, and their couplings are λ_3 independent.

6 Conclusion

Future e^+e^- linear colliders will probably offer the cleanest environment to discover a heavy charged Higgs through pair production. We have calculated the corresponding one loop radiative corrections in the on-mass-shell scheme, concentrating mainly here on a comparison between the contributions of the Higgs sector in a general THDM-II or MSSM-like contexts, as well as on the model-independent soft photon contributions. We were lead to introduce a parameterization which allows a practical comparison between the two models and involves only one extra parameter (ex. λ_3) as compared to the MSSM. The soft photon contribution for this process is found to be substantial (about -20%) for moderate values of the soft-photon energy cut-off ΔE . If λ_3 takes its MSSM values the one-loop corrections turn out to be rather small (a few percent). Away from its MSSM values, λ_3 induces large effects, both for small and large $\tan\beta$. Those large corrections arise from the contributions of model-dependent vertices which enter both the final state vertex and the charged Higgs renormalization constant. We also illustrated the overall sensitivity to the charged Higgs mass, $\tan\beta$ and the c.m. energy.

In summary, the radiative corrections to the charged Higgs pair production in e^+e^- annihilation can be significant and should be included in any reliable analysis. Furthermore, the large model-dependent effects can help discriminate phenomenologically between a (softly broken) supersymmetric and a non-supersymmetric minimal Higgs sector, irrespective of direct evidence for the susy spectrum. The one-loop corrections of the full-fledged MSSM should be eventually included. However they would not change much the conclusions of this paper in as much as the supersymmetric partners remain sufficiently heavy.

Acknowledgment: We thank Michel Capdequi Peyranère for his critical reading of

the manuscript and also for his collaboration in the early stage of this work. We are particularly indebted to Arndt Kraft for pointing out some errors in previously published results and helping us correct them.

AA acknowledges a research grant from Camões Institut of Lisbonne and thanks the departamento de Fisica-Centra, Instituto Superior Tecnico for the warm hospitality during his visit where part of this work has been done.

References

- [1] H.E. Haber and G.L. Kane, Phys. Rep. **117** (1985) p75.
H.P. Nilles, Phys. Rep.**110** (1984) 1;
P. Nath, R. Arnowitt and A. Chamseddine, “Applied N=1 Supergravity”, ITCP Series in Theoretical Physics, World Scientific, Singapore 1984;
X.R. Tata, in Proceedings of the “Mt Sorak Symposium on the Standard Model and Beyond”, Mt Sorak, Korea, 1990;
- [2] J.P. Derendinger and C.A. Savoy, N. Phys. **B237** (1984) 307, J. Ellis, J.F. Gunion, H.E. Haber, L. Roszkowski, F. Zwirner, Phys. Rev. D39 (1989) 844, U. Ellwanger, M. Rausch de Traubenberg, Z. Phys. **C53** (1992) 521
- [3] J.L. Feng, M.E. Peskin, H. Murayama, X. Tata Phys.Rev. **D52**, (1995) p1418-1432.
- [4] H.E.Haber and R.Hempfling, Phys. Rev. Lett.**66** , (1991), p1815.
Y.Okada, M.Yamaguchi and T.Yanagida, Prog. Theor. Phys. Lett. **85**, (1991) p1.
J.Ellis, G.Ridolfi and F.Zwirner, Phys.Lett. **B257** (1991) p83.
for further references see the talk by F.Zwirner, CERN-TH-6792-93.
- [5] M. Carena, M. Quiros and C. E. M. Wagner, Nucl. Phys. **B461**, (1996), p407.
H. E. Haber, R. Hempfling and A. H. Hoang, Z. Phys. **C75** (1997) p539.
- [6] J.F. Gunion, A. Turski Phys.Rev. **D40**: 2333, 1989; J.F. Gunion, A. Turski Phys.Rev. **D39** : 2701, 1989.
- [7] D. M. Pierce, J. A. Bagger, K. T. Matchev, and R-J Zhang, Nucl. Phys. **B491**, (1997), p3.
- [8] A.Brignole et al., Phys.Lett. **B271** (1991) 123; B273 (1991) 550(E);
M.A.Diaz and H.E.Haber, Phys.Rev. **D45** (1992) 4246;
P.H.Chankowski, S.Pokorski and J.Rosiek, Phys.Lett.**B274** (1992) 191;
A.Brignole, Phys.Lett. **B277** (1992) 313;
- [9] R. A. Jimenez, J. Sola, Phys. Lett. **B389**, (1996) p53.
A. Bartl, H. Eberl, K. Hidaka, T. Kon, W. Majerotto and Y. Yamada, Phys.Lett. **B378**, (1996), p167.
- [10] K. Ackerstaff et al, The OPAL Collaboration, Phys.Lett. **B426** (1998) p180. P. Abreu et al, DELPHI Collaboration Phys.Lett. **B420** (1998) p140 and R. Barate et al, ALEPH Collaboration, Phys.Lett. **B418** (1998) p419.
- [11] F. Abe et al, CDF Collaboration Phys.Rev.Lett. **79**: (1997) p357; *ibid.*, Phys. Rev. **D54**, (1996) p735; *ibid.*, Phys. Rev. Lett. **73** (1996) p2667.

- [12] D.P. Roy *hep-ph* 9704442, presented at the 32nd Rencontres de Moriond ,
M. Guchait and D.P. Roy, Phys. Rev. **D55**, (1997), p7263;
CDF Collaboration (F. Abe et al.) Phys.Rev.Lett. **79**: 357-362, 1997 (hep-
ex/9704003)
- [13] F. M. Borzumati and A. Djouadi *hep-ph* 9806301 and references therein.
- [14] T.G. Rizzo, Phys. Rev. **D 38** (1988) 820;
W.-S. Hou and R.S. Wiley, Phys. Lett. **B 302** (1988) 591;
C.Q. Geng and J.N. Ng, Phys. Rev. **D 38** (1988) 2857;
V. Barger, J.L. Hewet and R.J.N. Phillips, Phys. Rev. **D 41** (1990) 269.
- [15] M. Ciuchini, G. Degrassi, P. Gambino and G.F. Giudici *hep-ph*/9710335;
F. M. Borzumati and C. Greub, *hep-ph*/9802391;
- [16] T. Goto , Y. Okada, Prog.Theor.Phys.Suppl.123 (1996) **213**; and Prog.Theor.Phys.
94 (1995) 407.
- [17] Jiang Yi et al Journ. Phys **G23** (1997) p325, G24 (1998) p83, S. S. D. Willenbrock,
Phys. Rev. **D35** (1987) p173 and A. Krause, T. Plehn, M. Spira and P. M. Zerwas,
Nucl.Phys. B519 (1998) 85-100
- [18] V. Barger and R.J.N. Phillips, Phys. Rev. **D41**, (1990) p884; A. C. Bawa, C.S. Kim
and A. D. Martin, Z. Phys. **C47**, (1990) p75; R.M. Godbole and D.P. Roy Phys. Rev.
D43, (1991) p3640; M. Drees and D.P. Roy Phys. Lett. **B269**, (1991) p155.
- [19] V. Barger, R.J.N. Phillips and D. P. Roy, Lett. **B324**, (1994) p236;
J. F. Gunion, H. E. Haber, F. E. Paige, W. K. Tung and S. S. D. Willenbrock, Nucl.
Phys. **B294**, 621 (1987); R. M. Barnett, H. E. Haber and D. E. Soper, Nucl. Phys.
B306, (1988) p697; F. I. Olness and W. K. Tung, Nucl. Phys. **B308**, (1988) p813.
J. L. Diaz-Cruz and O. A. Sampayo, Phys. Rev. **D50**, (1994) p6820
S. Moretti and K. Odagiri, Phys. Rev. **D55**, (1997) p5627
- [20] D. A. Dicus, J. L. Hewtt, C. Kao and T. G. Rizzo, Phys. Rev. **D40** (1989) p787
A. A. Barrientos Bendezu and B. A. Kniehl, MPI/PhT/98-054 hep-ph/9807480
- [21] S. Komamiya, Phys. Rev. **D38** (1988) 2158;
- [22] A. Arhrib, M. Capdequi Peyranère, W. Hollik and G. Moultaka in preparation
- [23] A. Arhrib, M. Capdequi Peyranère and G. Moultaka, Phys. Lett. **B341**, p313–324,
(1995); Marco A. Diaz and Tonnies A. ter Veldhuis, hep-ph/9501315, DPF94 proceed-
ings;
- [24] A. Arhrib, G. Moultaka Proceedings of the Physics with e^+e^- Linear Colliders Work-
shop, Annecy–Gran Sasso–Hamburg 1995, ed. P. Zerwas (hep-ph/9606300).

- [25] D. Bowser–Chao et al, Phys. Lett. **B315** (1995) p 313; W. G. Ma et al Phys. Rev. **D53** (1996) p1304 and Shou Hua Zhu, Chong Sheng Li and Chong Shou Gao hep-ph/9712367.
- [26] J. F. Gunion and H. E. Haber, Nucl.Phys. **B272** (1986) 1 and ERRATA hep-ph/9301205;
- [27] H. Komatsu and J. Kubo, Phys. Lett. **B157** (1985) 90; Nucl. Phys. **B263** (1986) 265;
- [28] J. F. Gunion and H. E. Haber, Nucl. Phys. **B278**: 449, 1986 and ERRATA hep-ph/9301205;
- [29] For a review see e.g. J.F. Gunion, H.E. Haber, G.L. Kane and S. Dawson, The Higgs hunter’s guide (Addison-Wesley, Redwood City, 1990) and ERRATA SCIPP-92/58 (Dec. 92)
- [30] S.Glashow et S.Weinberg, Phys.Rev. **D15** (1977) p1958.
- [31] H.Eck and J. Kublbeck, Guide to FeynArts 1.0, University of Wurzburg, 1992.
R.Mertig, Guide to FeynCalc 1.0, University of Wurzburg, 1992.
- [32] A.Arhib, thesis , University Montpellier II(1994) Unpublished;
- [33] G.J. van Oldenborgh, Comput.Phys.Commun. **66** (1991) 1;
- [34] M.Böhm, W.Hollik and H.Spiesberger, Fortschr.Phys.**34** (1986) 11;
- [35] A. Dabelstein and W. Hollik MPI-PH-93-86, Contributed to Workshop on e+ e- Collisions at 500 GeV: the Physics Potential. Published in SUSY 94 Workshop:109-118 A. Dabelstein Z.Phys. **C67**,(1995), p495 and P. Chankowski, S. Pokorski and J. Rosiek Nucl.Phys.**B423**: 437-496,(1994)
- [36] OPAL Collaboration. Phys.Lett. **B370** (1996) p174 and R. M. Barnett et al. Phys. Rev. **D54** (1996) p1.
- [37] H. Burkhardt, F. Jegerlehner, G. Penso et C. Verzegnassi, Z. Phys. **C43** (1989) 497.
F. Jegerlehner, in Proc. 1990. Theoretical advanced study institute in elementary particle physics, eds. M. Cvetcic and P. Langacker, World scientific, Singapore (1991) 476. and hep-ph: 9502298.
A. D. Martin and D. Zeppenfeld Phys. Lett **B345** (1995), p558
- [38] A. Dabelstein Z.Phys.**C67**,(1995), p495 and P. Chankowski, S. Pokorski and J. Rosiek Nucl.Phys.**B423**: 437-496,(1994)
- [39] W. Hollik and C. Schappacher, KA–TP–3–1998 hep-ph/9807426

Table Captions:

Tab. 1: Soft photon contributions to the corrected cross section (in percent) and to the forward-backward asymmetry with the following cut-off on the photon energy:

$$\Delta E_1 = 0.05\sqrt{s}/2 \quad , \quad \Delta E_2 = 0.1\sqrt{s}/2 \quad , \quad \Delta E_3 = 0.15\sqrt{s}/2$$

Tab. 2: Fermionic (leptons+light quarks+top-bottom) contributions to the corrected cross section (in percent) for $m_{top} = 180 \text{ GeV}$.

Figure Captions:

Fig. 1: Feynman diagrams relevant for the $\mathcal{O}(\alpha)$ contributions to $e^+e^- \rightarrow H^+H^-$. 1. 1) s-channel self energy diagrams, 1.2–1.4) s-channel initial state vertex diagrams, 1.5–1.12) s-channel final state vertex diagrams, 1.13–1.14) THDM-II boxes diagrams, 1.17–1.21 Bremsstrahlung diagrams, 1.22–1.28) diagrams with a virtual photon and 1.29–1.33) self energy of the charged Higgs bosons necessary for the counterterms.

Fig. 2: Integrated tree level cross section as a function of m_{H^\pm} for three value of $\sqrt{s} = 500\text{GeV}$, 1000GeV and 1500GeV .

Fig. 3: Bosonic contribution (not including virtual and soft-photon emission) to the integrated cross section as a function of \sqrt{s} for $m_{H^\pm} = 220\text{GeV}$, 3.a) $\tan\beta = 2$ and severals values for λ_3 , 3.b) $\tan\beta = 30$ and severals values for λ_3

Fig. 4: Same as in Fig.3 with $m_{H^\pm} = 420\text{GeV}$

Fig. 5: Same as in Fig.3 with $m_{H^\pm} = 730\text{GeV}$

Fig. 6: Bosonic contribution (in percent) to the integrated cross section as a function of $\tan\beta$, a) $m_{H^\pm} = 220\text{GeV}$, $\sqrt{s} = 500\text{GeV}$ and different choices for λ_3 , b) $m_{H^\pm} = 300\text{GeV}$, $\sqrt{s} = 1000\text{GeV}$ and different choices for λ_3 , c) $m_{H^\pm} = 420\text{GeV}$, $\sqrt{s} = 1000\text{GeV}$...

Fig. 7: Standard box contributions to forward-Backward asymmetry as function of \sqrt{s} with $m_{H^\pm} = 220\text{GeV}$, $\tan\beta = 2$ and for several values of λ_3 around λ_3^{MSSM}

Fig. 8: Total one loop cross section σ_1 (in fb) as a function of \sqrt{s} for $m_{top} = 180\text{GeV}$ and $m_{H^\pm} = 220\text{GeV}$, 8. a) $\tan\beta = 2$, $\lambda_3 = \lambda_3^{MSSM} = -0.72$, $\lambda_3 = -1.2$ and $\lambda_3 = 0.05$, 8. b) $\tan\beta = 30$, $\lambda_3 = \lambda_3^{MSSM} = -0.72$, $\lambda_3 = -0.84$ and $\lambda_3 = -0.8$.

Fig. 9: Total one loop cross section σ_1 (in fb) as a function of \sqrt{s} for $m_{top} = 180\text{GeV}$ and $m_{H^\pm} = 420\text{GeV}$, 9. a) $\tan\beta = 2$, $\lambda_3 = \lambda_3^{MSSM} = -2.71$, $\lambda_3 = -3.6$ and $\lambda_3 = -1.8$, 9. b) $\tan\beta = 30$, $\lambda_3 = \lambda_3^{MSSM} = -2.71$, $\lambda_3 = -2.9$ and $\lambda_3 = -2.62$.

\sqrt{s}	500GeV		1 TeV		1.5 TeV	
$m_{H^+} GeV$	170	220	300	420	500	680
$\delta_{soft}^{\gamma}(\Delta E_1)(\%)$	-25.9	-24.7	-27.6	-26.4	-28.2	-26.5
$\delta_{soft}^{\gamma}(\Delta E_2)(\%)$	-17.	-15.9	-18.2	-17.2	-18.6	-17.2
$\delta_{soft}^{\gamma}(\Delta E_3)(\%)$	-11.8	-10.8	-12.7	-11.9	-12.9	-11.7
$A_{FB_{soft}}^{\gamma}(\Delta E_1)$	0.028	0.017	0.033	0.021	0.031	0.0164
$A_{FB_{soft}}^{\gamma}(\Delta E_2)$	0.0203	0.013	0.024	0.0151	0.0223	0.012
$A_{FB_{soft}}^{\gamma}(\Delta E_3)$	0.0166	0.01	0.0193	0.0124	0.0183	0.0097

Table 1.

\sqrt{s}	500GeV		1 TeV		1.5 TeV	
$(m_{H^+}(GeV), \tan\beta)$	(170,0.7)	(220,0.7)	(300, 0.7)	(420,0.7)	(500,0.7)	(680,0.7)
$\delta_{light-fermions}(\%)$	17.	17	18.7	18.7	19.8	19.8
$\delta_{top-bottom}(\%)$	-19.4	-24.6	-22.9	-16.5	-17.5	-13.6
$\delta_{total-fermions}(\%)$	-2.45	-7.4	-4.2	2.3	2.25	6.2
$(m_{H^+}(GeV), \tan\beta)$	(170,2)	(220,2)	(300, 2)	(420,2)	(500,2)	(680,2)
$\delta_{light-fermions}(\%)$	17.	17	18.7	18.7	19.8	19.8
$\delta_{top-bottom}(\%)$	-05.9	-06.6	-05.7	-04.9	-04.7	-04.2
$\delta_{total-fermions}(\%)$	11.	10.3	13.	13.8	15.1	15.6
$(m_{H^+}(GeV), \tan\beta)$	(170,10)	(220,10)	(300, 10)	(420,10)	(500,10)	(680,10)
$\delta_{light-fermions}(\%)$	17.	17.	18.7	18.7	19.7	19.7
$\delta_{top-bottom}(\%)$	-04.6	-04.8	-04.	-03.7	-03.4	-03.3
$\delta_{total-fermions}(\%)$	12.3	12.1	14.7	15.	16.3	16.5
$(m_{H^+}(GeV), \tan\beta)$	(170,20)	(220,20)	(300,20)	(420,20)	(500,20)	(680,20)
$\delta_{light-fermions}(\%)$	16.7	16.9	18.6	18.6	19.7	19.7
$\delta_{top-bottom}(\%)$	-05.8	-06.6	-05.8	-05.	-04.8	-04.3
$\delta_{total-fermions}(\%)$	10.9	10.3	12.8	13.6	14.9	15.4
$(m_{H^+}(GeV), \tan\beta)$	(170,30)	(220,30)	(300, 30)	(420,30)	(500,30)	(680,30)
$\delta_{light-fermions}(\%)$	16.8	16.8	18.5	18.6	19.6	19.6
$\delta_{top-bottom}(\%)$	-08.	-09.7	-08.9	-07.1	-07.1	-06.
$\delta_{total-fermions}(\%)$	08.8	07.1	09.6	11.5	12.5	13.6
$(m_{H^+}(GeV), \tan\beta)$	(170,60)	(220,60)	(300, 60)	(420,60)	(500,60)	(680,60)
$\delta_{light-fermions}(\%)$	16.2	16.3	17.8	18.1	18.9	19.2
$\delta_{top-bottom}(\%)$	-19.5	-26.3	-26.	-18.5	-19.9	-15.3
$\delta_{total-fermions}(\%)$	-3.3	-9.9	-8.1	-0.04	-1.	3.8

Table 2.

Appendix

Appendix A: Couplings

For completeness, we give in this section the Feynman rules of the 3-point vertices involving the charged Higgs in the general THDM, in two different forms.

In terms of the λ_i 's, α and β , one has

$$g_{H^0 H^+ H^-} = -i\sqrt{2}v \left[-\frac{\lambda_5}{2} \sin 2\beta \sin(\alpha + \beta) + (\lambda_4 + 2\lambda_3) \cos(\beta - \alpha) \right. \\ \left. + \sin 2\beta (\lambda_2 \sin \alpha \cos \beta + \lambda_1 \cos \alpha \sin \beta) \right] \quad (\text{A.1})$$

$$g_{h^0 H^+ H^-} = -i\sqrt{2}v \left[-\frac{\lambda_5}{2} \sin 2\beta \cos(\alpha + \beta) + (\lambda_4 + 2\lambda_3) \sin(\beta - \alpha) \right. \\ \left. + \sin 2\beta (\lambda_2 \cos \alpha \cos \beta - \lambda_1 \sin \alpha \sin \beta) \right] \quad (\text{A.2})$$

$$g_{H^0 H^\pm G^\mp} = -\frac{iv}{\sqrt{2}} \left[(\lambda_5 - \lambda_4) \cos 2\beta \sin(\alpha + \beta) + \lambda_4 \sin 2\beta \cos(\alpha + \beta) \right. \\ \left. + 2 \sin 2\beta (\lambda_2 \sin \alpha \sin \beta - \lambda_1 \cos \alpha \cos \beta) \right] \\ = \frac{-ig \sin(\beta - \alpha)(m_{H^\pm}^2 - m_H^2)}{2m_W} \quad (\text{A.3})$$

$$g_{h^0 H^\pm G^\mp} = -\frac{iv}{\sqrt{2}} \left[(\lambda_5 - \lambda_4) \cos 2\beta \cos(\alpha + \beta) - \lambda_4 \sin 2\beta \sin(\alpha + \beta) \right. \\ \left. + 2 \sin 2\beta (\lambda_2 \cos \alpha \sin \beta + \lambda_1 \sin \alpha \cos \beta) \right] \\ = \frac{ig \cos(\beta - \alpha)(m_{H^\pm}^2 - m_h^2)}{2m_W} \quad (\text{A.4})$$

$$g_{A^0 H^\pm G^\mp} = \mp \frac{v}{\sqrt{2}} (\lambda_6 - \lambda_4) = \mp \frac{m_{H^\pm}^2 - m_A^2}{v\sqrt{2}} \quad (\text{A.5})$$

where the trigonometric functions of α should be expressed further in terms of the λ_i 's and $\tan \beta$, using eqs.(3,4) with

$$v_1 = \frac{v}{\sqrt{1 + \tan^2 \beta}} \quad v_2 = v \sqrt{\frac{\tan^2 \beta}{(1 + \tan^2 \beta)}}$$

Another useful form is in terms of deviations from the MSSM tree-level mass-sum-rules. Defining

$$\lambda_3 = \frac{1}{8}(g^2 + g'^2) - \lambda_1 + \frac{m_W^2}{v^2} \delta_3 \quad (\text{A.6})$$

$$m_{H^\pm}^2 = (m_{H^\pm}^2)_{MSSM} + m_W^2 \delta_\pm \quad (\text{A.7})$$

$$m_H^2 = (m_H^2)_{MSSM} + m_W^2 \delta_H \quad (\text{A.8})$$

$$m_h^2 = (m_h^2)_{MSSM} + m_W^2 \delta_h \quad (\text{A.9})$$

where $(m_{H^\pm}^2)_{MSSM}$ and $(m_{H/h}^2)_{MSSM}$ are given by eqs.(17, 18), then the Feynman rules for the vertices $H_0 H^+ H^-$ and $h_0 H^+ H^-$ read

$$g_{H^0 H^+ H^-} = g_{H^0 H^+ H^-}^{MSSM} - i g m_W [\cos(\beta - \alpha) (\delta_\pm - \frac{\delta_H}{2}) + \frac{\sin(\alpha + \beta)}{\sin 2\beta \tan^2 \beta} \{4\delta_3 - \frac{1}{2}(\delta_H + \delta_h) - \frac{1}{2\cos^3 \beta} (\cos(2\alpha + \beta) + \sin \beta (\frac{\sin 2\alpha}{2} + \sin(\alpha - \beta) \cos(\alpha + \beta))) (\delta_H - \delta_h)\}] \quad (\text{A.10})$$

$$g_{h^0 H^+ H^-} = g_{h^0 H^+ H^-}^{MSSM} - i g m_W [\sin(\beta - \alpha) (\delta_\pm - \frac{\delta_H}{2}) + \frac{\cos(\alpha + \beta)}{\sin 2\beta \tan^2 \beta} \{4\delta_3 - \frac{1}{2}(\delta_H + \delta_h) - \frac{1}{2\cos^3 \beta} (\cos(2\alpha + \beta) + \sin \beta (\frac{\sin 2\alpha}{2} + \sin(\alpha + \beta) \cos(\alpha - \beta))) (\delta_H - \delta_h)\}] \quad (\text{A.11})$$

It's interesting to note that in the general THDM the big effects (in the case where $\tan\beta$ is large or very small) comes from the δ_3 or $\delta_{H,h}$ but never from δ_\pm . Note also that these effects are not present not only in the susy case but also when $\delta_H = \delta_h = 4\delta_3$.

Appendix B: Passarino–Veltman Functions

Let us recall the definitions of scalar and tensor integrals we use: The inverse of the propagators are denoted by

$$D_0 = q^2 - m_0^2, \quad D_i = (q + p_i)^2 - m_i^2$$

Where the p_i are the momentum of the external particles.

One point functions:

$$A_0(m_0^2) = \frac{1}{i\pi^2} \int d^n q \frac{1}{D_0}$$

Two point functions:

$$B_{0,\mu}(p_1^2, m_0^2, m_1^2) = \frac{1}{i\pi^2} \int d^n q \frac{1, q_\mu}{D_0 D_1}$$

using Lorentz invariance, we have:

$$B_\mu = p_{1\mu} B_1$$

Three point functions:

$$C_{0,\mu,\mu\nu}(p_1^2, p_{12}^2, p_2^2, m_0^2, m_1^2, m_2^2) = \frac{1}{i\pi^2} \int d^n q \frac{1, q_\mu, q_\mu q_\nu}{D_0 D_1 D_2}$$

using Lorentz invariance, we have:

$$C_\mu = p_{1\mu} C_1 + p_{2\mu} C_2 \quad (\text{B.1})$$

$$C_{\mu\nu} = g_{\mu\nu} C_{00} + p_{1\mu} p_{1\nu} C_{11} + p_{2\mu} p_{2\nu} C_{22} + (p_{1\mu} p_{2\nu} + p_{2\mu} p_{1\nu}) C_{12} \quad (\text{B.2})$$

Four point functions:

$$D_{0,\mu,\mu\nu}(p_1^2, p_{12}^2, p_{23}^2, p_3^2, p_2^2, p_{13}^2, m_0^2, m_1^2, m_2^2, m_3^2) = \frac{1}{i\pi^2} \int d^n q \frac{1, q_\mu, q_\mu q_\nu}{D_0 D_1 D_2 D_3} \quad (\text{B.3})$$

using Lorentz invariance, we have:

$$D_\mu = p_{1\mu} D_1 + p_{2\mu} D_2 + p_{3\mu} D_3 \quad (\text{B.4})$$

$$\begin{aligned} D_{\mu\nu} = & g_{\mu\nu} D_{00} + p_{1\mu} p_{1\nu} D_{11} + p_{2\mu} p_{2\nu} D_{22} + p_{3\mu} p_{3\nu} D_{33} + (p_{1\mu} p_{2\nu} + p_{2\mu} p_{1\nu}) D_{12} \\ & + (p_{1\mu} p_{3\nu} + p_{3\mu} p_{1\nu}) D_{13} + (p_{3\mu} p_{2\nu} + p_{2\mu} p_{3\nu}) D_{23} \end{aligned} \quad (\text{B.5})$$

Appendix C: Vertex amplitudes.

In this section we give only some typical amplitudes of the final state vertex contributions drawn in figure 1. The amplitude will be projected on the two invariants I_V and I_A defined in section 3.

The s-channel self-energy $\gamma\text{--}\gamma$, $\gamma\text{--}Z$ and $Z\text{--}Z$ can be found in [38], [39] The standard model initial state vertex contributions Fig 1.2, 1.3 and 1.4 are well known and will not be given here.

The remaining amplitudes are given as follow:

Diagram 1.5

$$\begin{aligned} \mathcal{M}_{1.5} = & \frac{\alpha^2 g_{SH+W} g_{SH-W} + g_{VW+W-}}{(s - m_V^2)} \left(4 B_0(s, m_W^2, m_W^2) + (4m_S^2 + s) C_0 - 4 s C_1 \right. \\ & \left. - 4 C_{00} + 2 s \kappa^2 (C_{11} + C_{12}) \right) (g_V I_V - g_A I_A) \end{aligned} \quad (\text{C.1})$$

Where $g_{ZW^+W^-} = \frac{c_W}{s_W}$, $g_{\gamma W^+W^-} = 1$, $g_{H_0 H^\mp W^\pm} = \pm \frac{1}{2s_W} s_{\beta\alpha}$,

$g_{h_0 H^\mp W^\pm} = \mp \frac{1}{2s_W} c_{\beta\alpha}$, $g_{A_0 H^\mp W^\pm} = \frac{-i}{2s_W}$, with $\{c, s\}_{\beta\alpha} = \{\cos, \sin\}(\beta - \alpha)$ and $\kappa^2 = 1 - \frac{4m_{H^\pm}^2}{s}$ and m_S is the mass of the scalar particle S.

The C_i and C_{ij} have as arguments $(m_{H^\pm}^2, s, m_{H^\pm}^2, m_S^2, m_W^2, m_W^2)$.

Diagram 1.6

- $i \neq j$

$$\begin{aligned} \mathcal{M}_{1.6} = & 2 \frac{\alpha^2 g_V S_i S_j g_{V' S_i H^-} g_{V' S_j H^+}}{(s - m_{V'}^2)} \left((4 m_{H^\pm}^2 + m_{V'}^2 - 2 s) C_0 + 4 C_{00} \right. \\ & \left. + (8 m_{H^\pm}^2 + m_{V'}^2 - 3 s)(C_1 + C_2) - s \kappa^2 (C_{11} + 2 C_{12} + C_{22}) \right) (g_V I_V - g_A I_A) \end{aligned} \quad (C.2)$$

- $i = j$

$$\begin{aligned} \mathcal{M}_{1.6} = & 2 \frac{\alpha^2 g_V S_i S_i g_{V' S_i H^-} g_{V' S_i H^+}}{(s - m_{V'}^2)} \left((4 m_{H^\pm}^2 + m_{V'}^2 - 2 s) C_0 + 4 C_{00} + \right. \\ & \left. 2(8 m_{H^\pm}^2 + m_{V'}^2 - 3 s) C_1 - 2 s \kappa^2 (C_{11} + C_{12}) \right) (g_V I_V - g_A I_A) \end{aligned} \quad (C.3)$$

The C_i and C_{ij} have as arguments $(m_{H^\pm}^2, s, m_{H^\pm}^2, m_{V'}^2, m_{S_i}^2, m_{S_j}^2)$. the coupling constants being defined in the following table.

(S_i, S_j, V')	(H_0, A_0, W^+)	(h_0, A_0, W^+)	(H^+, H^-, Z)	(H^+, H^-, γ)
$g_Z S_i S_j$	$i \frac{s_{\beta\alpha}}{2s_W c_W}$	$-i \frac{c_{\beta\alpha}}{2s_W c_W}$	$-\frac{(c_W^2 - s_W^2)}{2s_W c_W}$	$-\frac{(c_W^2 - s_W^2)}{2s_W c_W}$
$g_\gamma S_i S_j$	0	0	-1	-1
$g_{H^\mp S_i V'}$	$\pm \frac{1}{2s_W} s_{\beta\alpha}$	$\mp \frac{1}{2s_W} c_{\beta\alpha}$	$-\frac{(c_W^2 - s_W^2)}{2s_W c_W}$	-1
$g_{H^\pm S_j V'}$	$\frac{\mp i}{2s_W}$	$\frac{\mp i}{2s_W}$	$-\frac{(c_W^2 - s_W^2)}{2s_W c_W}$	-1

where i, j label the five Higgs particles h_0, H_0, A_0, H^+, H^- . When V' is the photon, one has to keep consistently a photon mass regulator in

$C_0(m_{H^\pm}^2, m_{H^\pm}^2, s, m_{H^\pm}^2, m_{H^\pm}^2, m_{V'}^2)$ to account for the IR singularity, taking everywhere else in eq.(C.2) $m_{V'} \rightarrow 0$. Summation over all i, j should be understood for the full contribution of diagram 1.6.

Diagram 1.7 and 1.8

In this case: if V is the Z boson then V' is the Z boson (resp. W^\pm boson) and S_i is a neutral (resp. charged) Higgs boson while S_j is the charged (resp. neutral) one.

if V is the photon then V' is the W^\pm gauge boson and S_i is a charged Higgs boson while

S_j is the neutral one.

$$\mathcal{M}_{1.7} = -\frac{\alpha^2 g_{S_i S_j H^+} g_{V' S_j H^-} g_{VV' S_i}}{(s - m_V^2)} \left(C_0 - C_1 - C_2 \right) (g_V I_V - g_A I_A) \quad (\text{C.4})$$

C_i have as arguments $(m_{H^\pm}^2, s, m_{H^\pm}^2, m_{S_j}^2, m_{V'}^2, m_{S_i}^2)$

$$\mathcal{M}_{1.8} = -\frac{\alpha^2 g_{S_i S_j H^+} g_{V' S_j H^-} g_{VV' S_i}}{(s - m_V^2)} \left(C_0 - C_1 - C_2 \right) (g_V I_V - g_A I_A) \quad (\text{C.5})$$

C_i have as arguments $(m_{H^\pm}^2, s, m_{H^\pm}^2, m_{S_j}^2, m_{S_i}^2, m_{V'}^2)$

The coupling are given in the following table

(S_i, S_j, V')	(H_0, H^+, Z)	(h_0, H^+, Z)	(G^+, H_0, W^\pm)	(G^+, h_0, W^\pm)	(G^+, A_0, W^\pm)
$g_{ZV' S_i}$	$m_Z \frac{c_{\beta\alpha}}{s_W c_W}$	$m_Z \frac{s_{\beta\alpha}}{s_W c_W}$	$-m_Z s_W$	$-m_Z s_W$	$-m_Z s_W$
$g_{\gamma V' S_i}$	0	0	m_W	m_W	m_W
$g_{S_i S_j H^\mp}$	$-i g_{H_0 H^+ H^-}$	$-i g_{h_0 H^+ H^-}$	$-i g_{G^+ H_0 H^-}$	$-i g_{G^+ h_0 H^-}$	$i g_{A^0 G^\pm H^\mp}$
$g_{V' S_j H^\pm}$	$-\frac{(c_W^2 - s_W^2)}{2 s_W c_W}$	$-\frac{(c_W^2 - s_W^2)}{2 s_W c_W}$	$\pm \frac{1}{2 s_W} s_{\beta\alpha}$	$\mp \frac{1}{2 s_W} c_{\beta\alpha}$	$-i \frac{1}{2 s_W}$

where $g_{H_0 H^+ H^-}$, $g_{h_0 H^+ H^-}$, $g_{H_0 H^+ G^-}$ and $g_{h_0 H^+ G^-}$ are defined in appendix A. Summation over all i, j should be understood for the full contribution of diagrams 1.7 and 1.8.

Diagram 1.9

In the case of three different scalar S_i , S_j and S_k with $S_i \neq S_j$, only the Z boson is coupled to two different scalar (the coupling of the photon is forbidden because of the conservation of the electromagnetic current)

• $i \neq j$

$$\mathcal{M}_{1.9} = 2 \frac{\alpha^2 g_{H^+ S_j S_k} g_{H^- S_i S_k} g_{V S_i S_j}}{(s - m_V^2)} \left(C_0 + C_1 + C_2 \right) (g_V I_V - g_A I_A) \quad (\text{C.6})$$

• $i = j$

$$\mathcal{M}_{1.9} = 2 \frac{\alpha^2 g_{H^+ S_i S_k} g_{H^- S_i S_k} g_{V S_i S_i}}{(s - m_V^2)} \left(C_0 + 2C_1 \right) (g_V I_V - g_A I_A) \quad (\text{C.7})$$

Where C_i have as arguments: $(m_{H^\pm}^2, s, m_{H^\pm}^2, m_{S_k}^2, m_{S_j}^2, m_{S_i}^2)$

(S_i, S_j, S_k)	(H_0, A_0, G^+)	(h_0, A_0, G^+)
$g_{Z S_i S_j}$	$i \frac{s_{\beta\alpha}}{2 s_W c_W}$	$-i \frac{c_{\beta\alpha}}{2 s_W c_W}$
$g_{H^\pm S_j S_k}$	$i g_{A^0 G^\mp H^\pm}$	$i g_{A^0 G^\mp H^\pm}$
$g_{H^- S_i S_k}$	$-i g_{H_0 H^- G^+}$	$-i g_{h_0 H^- G^+}$

In this case, we have the following situation:

If $S_i = H^+$ then $V = \gamma$ or Z , $S_k = H_0$ or h_0 in this case we have $g_{ZH^+H^-} = -\frac{(c_W^2 - s_W^2)}{2s_W c_W}$, $g_{\gamma H^+H^-} = -1$. The coupling $g_{H_0 H^+ H^-}$ and $g_{h_0 H^+ H^-}$ are model dependent and are given in eqs. (A.10, A.11).

If $S_i = G^+$ then $V = \gamma$ or Z , $S_k = H_0, h_0$ or A_0 in this case we have $g_{ZG^+G^-} = -\frac{(c_W^2 - s_W^2)}{2s_W c_W}$, $g_{\gamma G^+G^-} = -1$. Summation over all i, j should be understood for the full contribution of diagram 1.9.

Diagram 1.10 and 1.11

The amplitude of diagram 1.10 is equal to the amplitude of 1.11.

$$\begin{aligned} \mathcal{M}_{1.10+1.11} &= \frac{\alpha^2 g_{VV'SH^-} g_{SH^+V'}}{2m_{H^\pm}^2 (s - m_{V'}^2)} ((m_S^2 - m_{V'}^2) B_0(0, m_S^2, m_{V'}^2) \\ &\quad + (-m_S^2 - 3m_{H^\pm}^2 + m_{V'}^2) B_0(m_{H^\pm}^2, m_S^2, m_{V'}^2)) (g_V I_V - g_A I_A) \end{aligned} \quad (C.8)$$

Where V denotes the photon or the Z gauge boson,

V' a charged (resp. neutral) gauge boson and S a neutral (resp. charged) scalar particle.

The couplings of these contributions are given by:

- $W^- H_0$ exchange:

$$\begin{aligned} V &= \text{photon}, g_{\gamma W^- H_0 H^+} = -\frac{1}{2s_W} s_{\beta\alpha}, g_{H_0 H^\mp W^\pm} = \pm \frac{1}{2s_W} s_{\beta\alpha} \\ V &= Z, g_{ZW^+ H_0 H^-} = \frac{1}{2c_W} s_{\beta\alpha} \end{aligned}$$

- $W^- h_0$ exchange:

$$\begin{aligned} V &= \text{photon}, g_{\gamma W^+ h_0 H^-} = \frac{1}{2s_W} c_{\beta\alpha}, g_{h_0 H^\mp W^\pm} = \mp \frac{1}{2s_W} c_{\beta\alpha} \\ V &= Z, g_{ZW^+ h_0 H^-} = -\frac{1}{2c_W} c_{\beta\alpha} \end{aligned}$$

- $W^- A_0$ exchange:

$$\begin{aligned} V &= \text{photon}, g_{\gamma W^+ A_0 H^-} = \frac{-i}{2s_W}, g_{A_0 H^\mp W^\pm} = \frac{-i}{2s_W}. \\ V &= Z, g_{ZW^+ A_0 H^-} = \frac{i}{2c_W} \end{aligned}$$

- $Z H^+$ exchange:

$$\begin{aligned} V &= \text{photon}, g_{\gamma ZH^+H^-} = \frac{c_W^2 - s_W^2}{s_W c_W}, g_{\gamma H^+H^-} = -1 \\ V &= Z, g_{ZZH^+H^-} = \frac{(c_W^2 - s_W^2)^2}{2s_W^2 c_W^2}, g_{ZH^+H^-} = -\frac{c_W^2 - s_W^2}{2s_W c_W} \end{aligned}$$

- photon H^+ exchange:

$$\begin{aligned} V &= \text{photon}, g_{\gamma\gamma H^+H^-} = 2, g_{\gamma H^+H^-} = -1 \\ V &= Z, g_{\gamma ZH^+H^-} = \frac{c_W^2 - s_W^2}{s_W c_W}, g_{\gamma H^+H^-} = -1 \end{aligned}$$

Diagram 1.12

For up-down exchange in the vertex the amplitude is given by:

- photon exchange:

$$\mathcal{M}_{1.12} = \frac{e_u N_C \alpha^2}{m_W^2 s_W^2 s} \left(2((m_d^2 + m_{H^\pm}^2 + m_u^2)(Y_u^2 + Y_d^2) + 4m_d m_u Y_u Y_d) C_1 + \right. \\ \left. 2(m_d^2(Y_u^2 + Y_d^2) + 2m_u m_d Y_u Y_d) C_0 + (Y_u^2 + Y_d^2) B_0(s, m_u^2, m_u^2) + \right) I_V \quad (\text{C.9})$$

- Z-exchange:

$$\mathcal{M}_{1.12} = \frac{-N_C \alpha^2}{2c_W m_W^2 (s - m_V^2) s_W^3} \left((2e_u s_W^2 (Y_u^2 + Y_d^2) - Y_d^2) B_0(s, m_u^2, m_u^2) + \right. \\ \left. \{4e_u s_W^2 ((Y_u^2 + Y_d^2) m_d^2 + 2m_u m_d Y_u Y_d) - 2m_u m_d Y_u Y_d - 2m_d^2 Y_d^2\} C_0 \right. \\ \left. - 2\{(m_u Y_u + m_d Y_d)^2 + m_{H^\pm}^2 Y_d^2 - 2e_u s_W^2 ((Y_u^2 + Y_d^2)(m_d^2 + m_{H^\pm}^2 + m_u^2) \right. \\ \left. + 4m_d m_u Y_u Y_d)\} C_1 \right) (g_V I_V - g_A I_A) \quad (\text{C.10})$$

The C_i have as arguments $(m_{H^\pm}^2, s, m_{H^\pm}^2, m_d^2, m_u^2, m_u^2)$ The contributions of the down-down-up vertex are obtained from the ones above through the replacement:

$$e_u \rightarrow -e_d, \quad Y_u \rightarrow Y_d, \quad Y_d \rightarrow Y_u, \quad m_u \rightarrow m_d, \quad m_d \rightarrow m_u$$

Appendix D: Box amplitudes.

In this section we give the box amplitudes both for standard and supersymmetric cases.

THDM-II boxes

We give the general amplitude for THDM-II boxes which are drawn in figure 1 (1.13, 1.14, 1.28, 1.29 and 1.30) with exchange of two gauge boson one scalar and one fermion. We denote by V_1 and V_2 the two gauge bosons with masses m_2 and m_4 , S a scalar particle with mass m_1 and l a lepton (electron or neutrino) with mass m_3 of which we keep trace only in the arguments of the Passarino-Veltman functions, and neglect otherwise.

We will use the following notations for the coupling:

- gauge boson-two scalars: $V_\mu S_1 S_2 = i e g_H (p - p')_\mu$
- gauge boson-two fermions: $V_\mu^i f f' = i e \gamma_\mu (g_{V_i} - g_{A_i} \gamma_5)$

we find then:

$$\mathcal{M}_{box} = \alpha^2 g_{H_1} g_{H_2} (G_V I_V - G_A I_A) INV$$

with :

$$G_A = g_{A_2} g_{V_1} + g_{A_1} g_{V_2}, \quad G_V = g_{A_1} g_{A_2} + g_{V_1} g_{V_2}$$

and

$$\begin{aligned} INV = & ((-4 C_0(m_e^2, m_e^2, s, m_2^2, m_1^2, m_4^2) - (3m_{H\pm}^2 - t) D_0 + 2 (-t + m_{H\pm}^2) D_1 + \\ & (-t + m_{H\pm}^2) D_2 + 2 (-t + m_{H\pm}^2) D_3 + 2 D_{00} + (m_{H\pm}^2 + t) D_{11} + 2 t D_{22} + \\ & (m_{H\pm}^2 + 3t) D_{12} + 2 (m_{H\pm}^2 + t) D_{13} + (m_{H\pm}^2 + 3t) D_{23} + (m_{H\pm}^2 + t) D_{33})) \quad (D.1) \end{aligned}$$

The D_0 , D_i $i = 1, 2, 3$ and D_{ij} have as arguments $(m_{H\pm}^2, m_e^2, m_e^2, m_{H\pm}^2, t, s, m_1^2, m_2^2, m_3^2, m_4^2)$.

In the case of exchange of neutral gauge bosons in the box, we have to add the crossed boxes. The amplitude can be deduced from the above one by changing t into u and a global sign.

In the case of photon exchange in the box we have to regularize the I.R divergence by a small mass. we have checked numerically and analytically that the I.R divergence cancels out when adding the soft photon Bremsstrahlung.

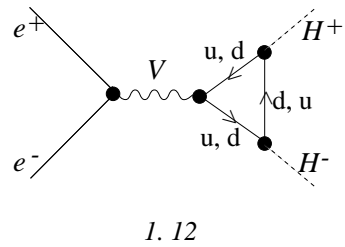
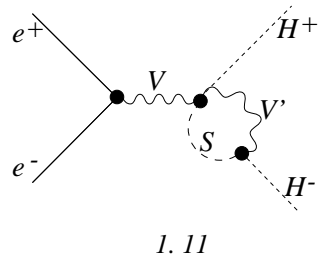
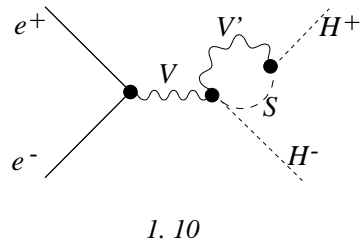
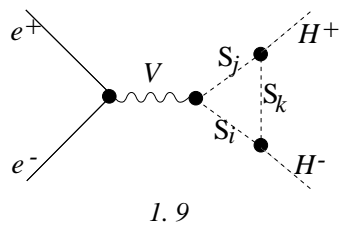
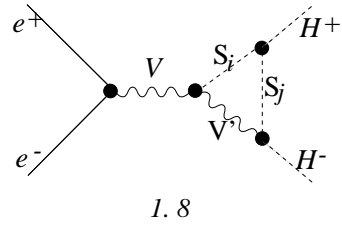
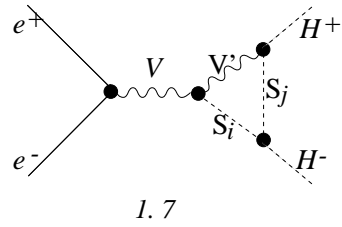
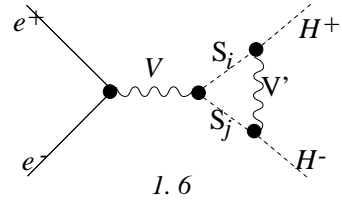
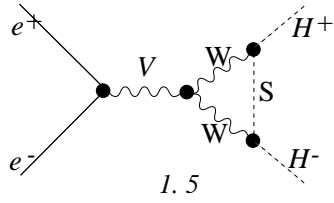
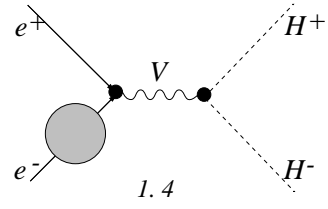
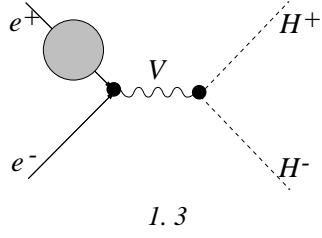
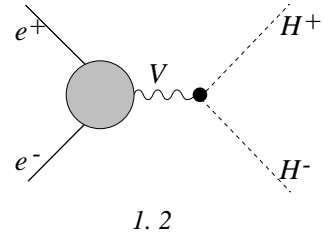
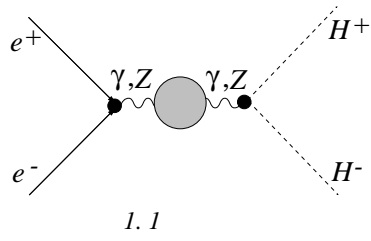
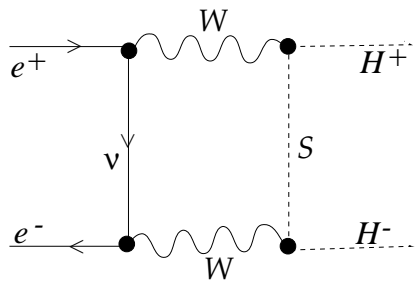
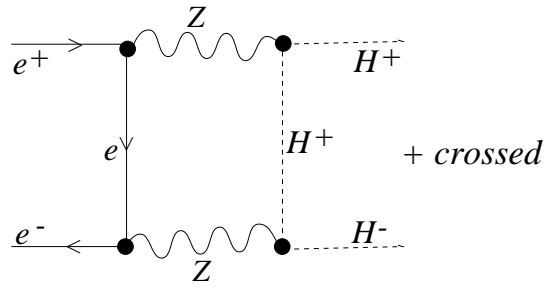


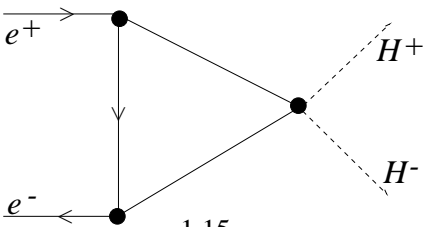
Fig 1



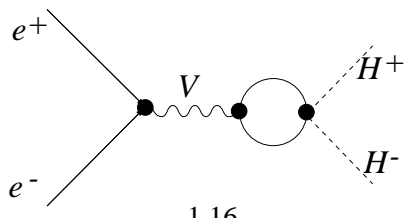
1.13



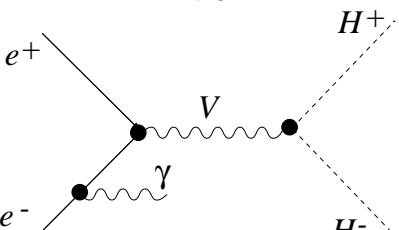
1.14



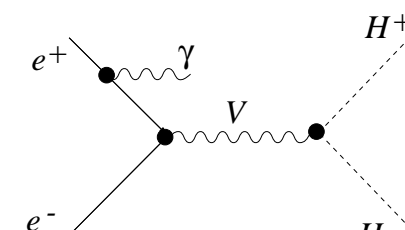
1.15



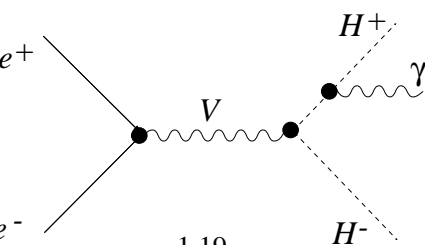
1.16



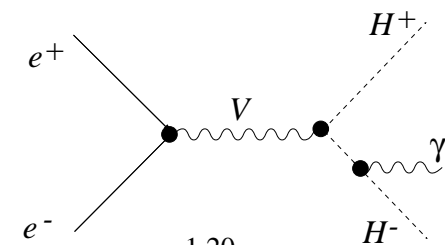
1.17



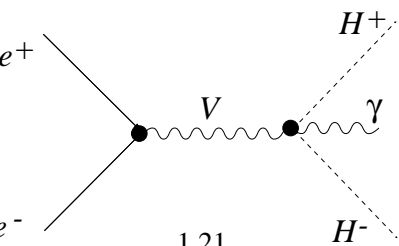
1.18



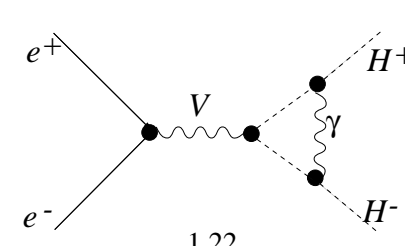
1.19



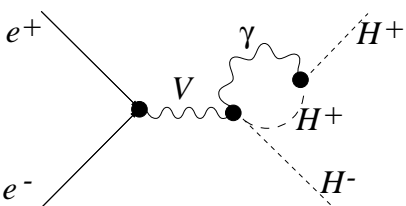
1.20



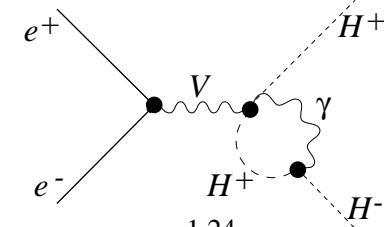
1.21



1.22

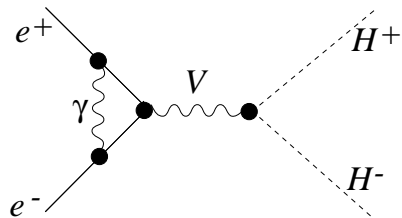


1.23

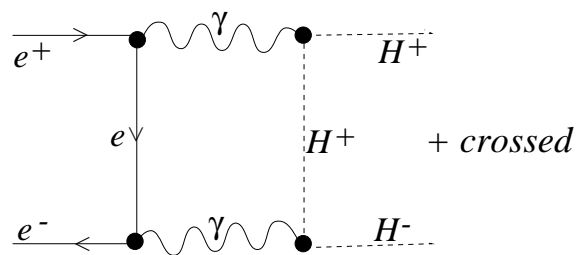


1.24

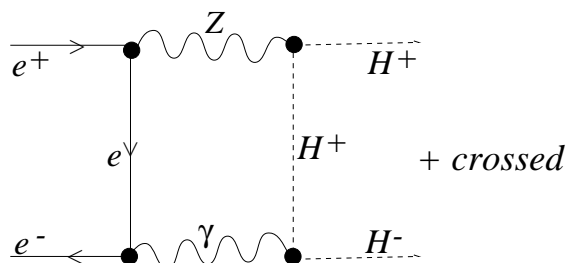
Fig 1 (cont.)



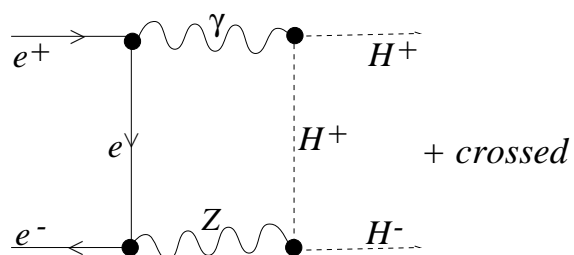
1.25



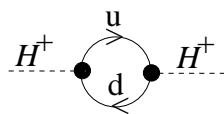
1.26



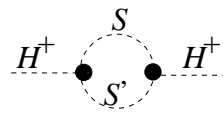
1.27



1.28



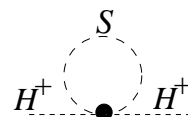
1.29



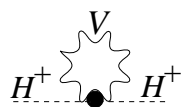
1.30



1.31



1.32



1.33

Fig 1 (cont.)

Fig. 2

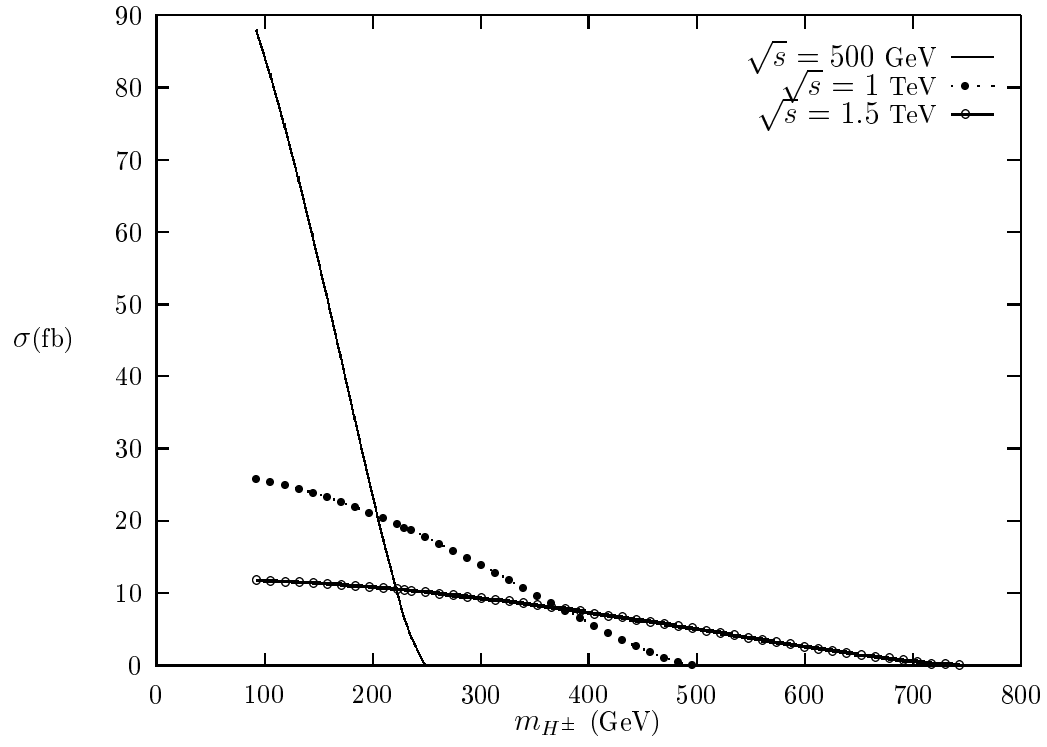


Fig 3. a

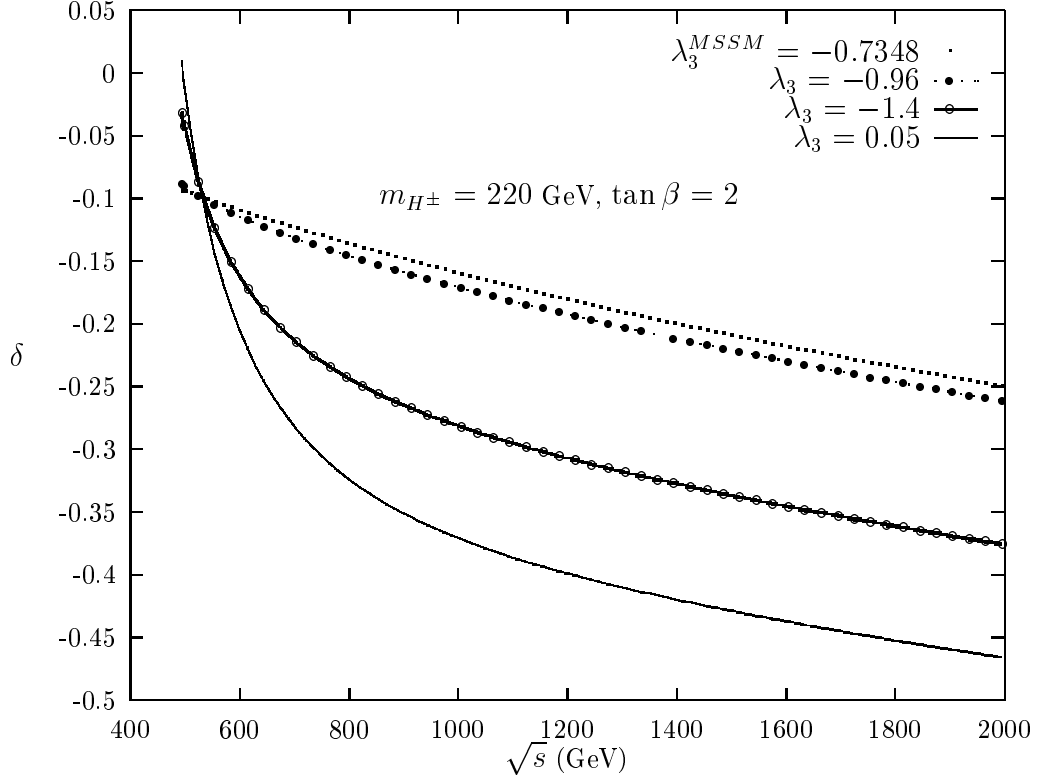


Fig 3. b

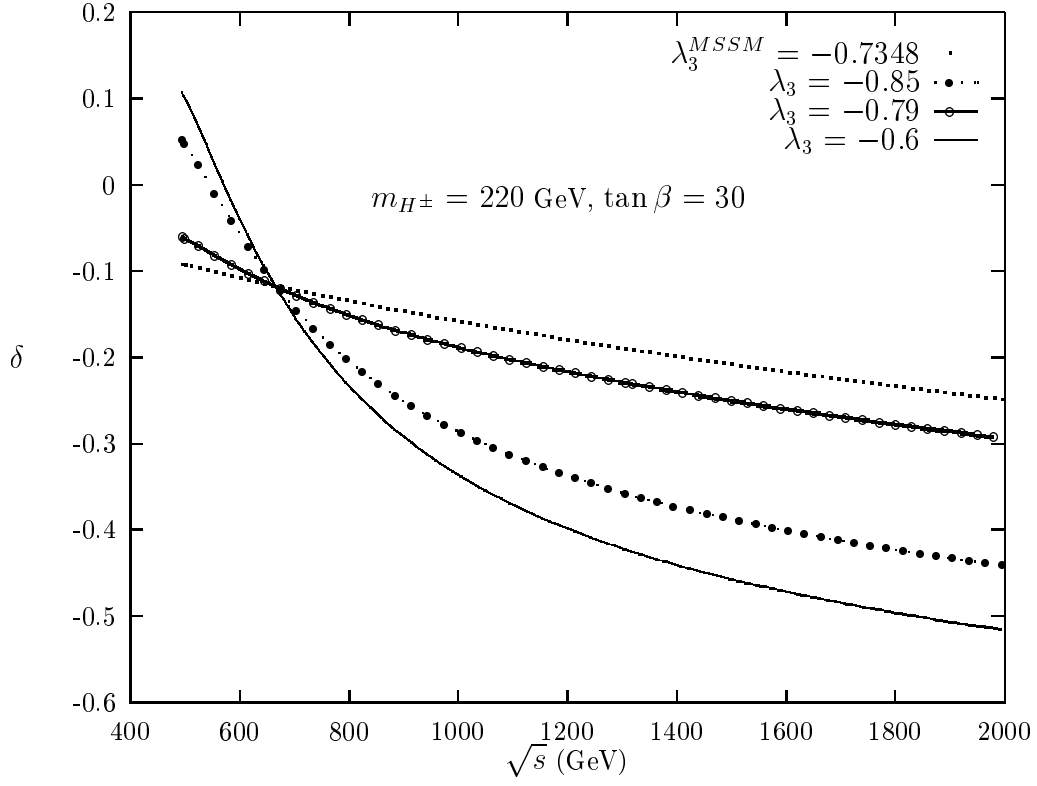


Figure. 3

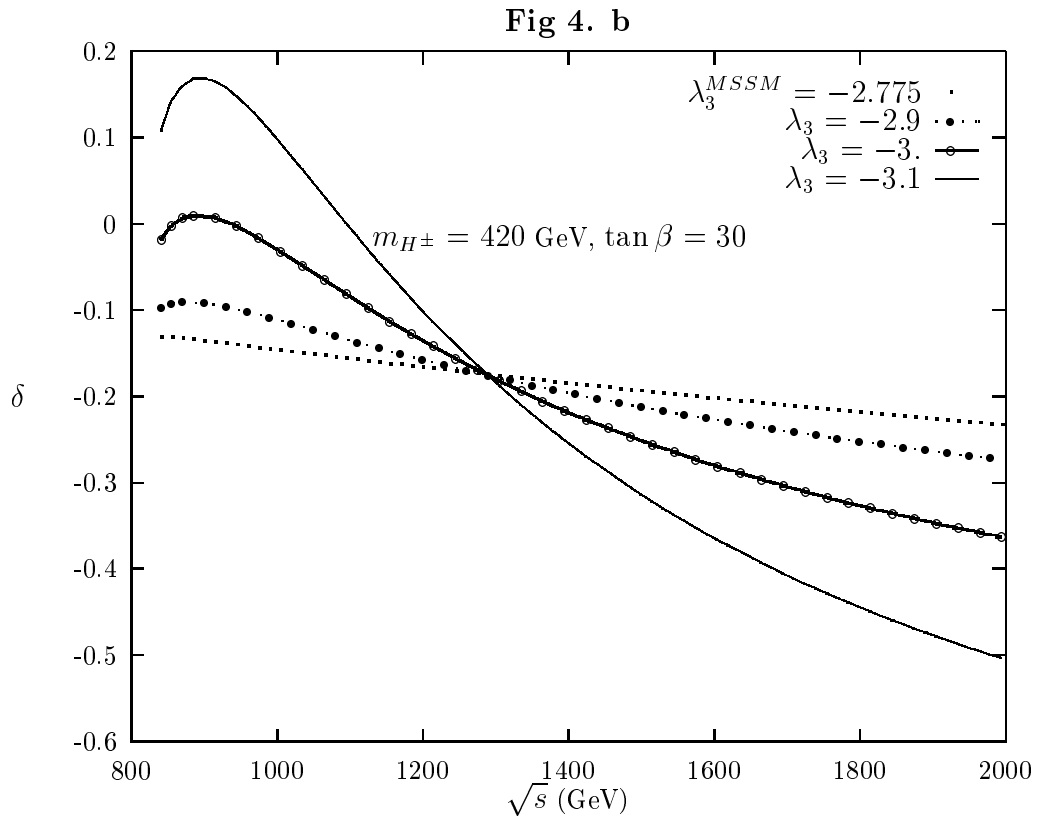
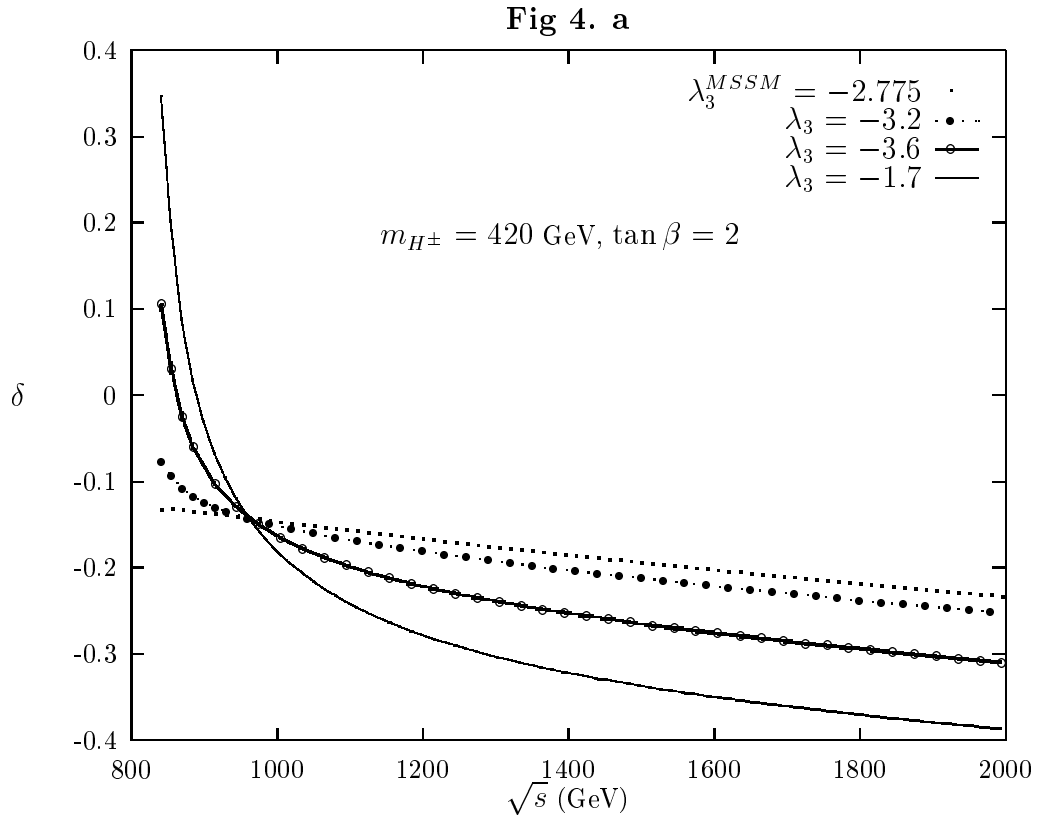


Figure. 4

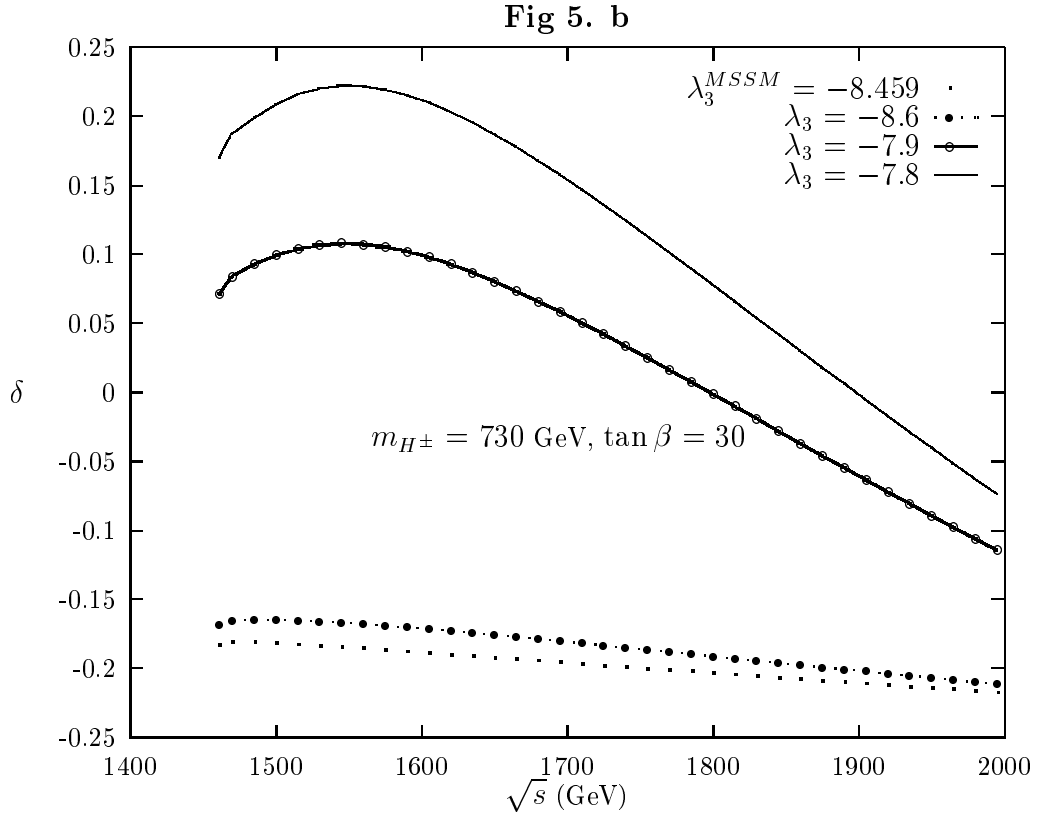
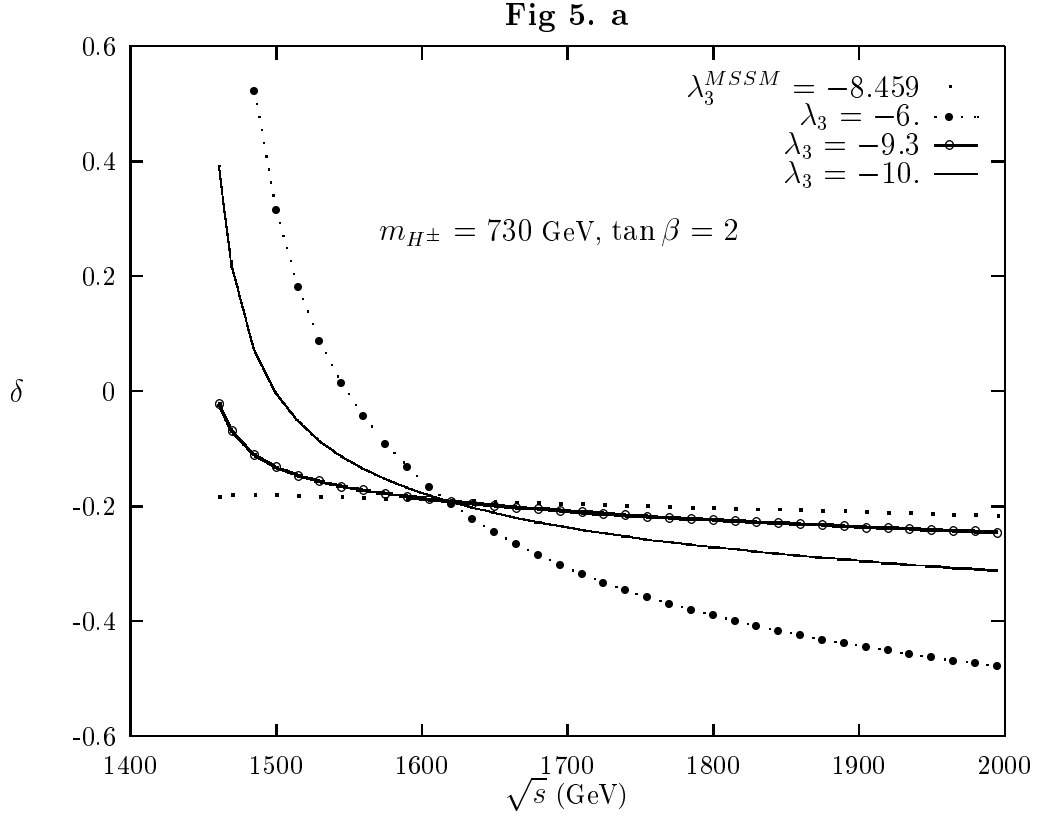


Figure. 5

Fig 6. a

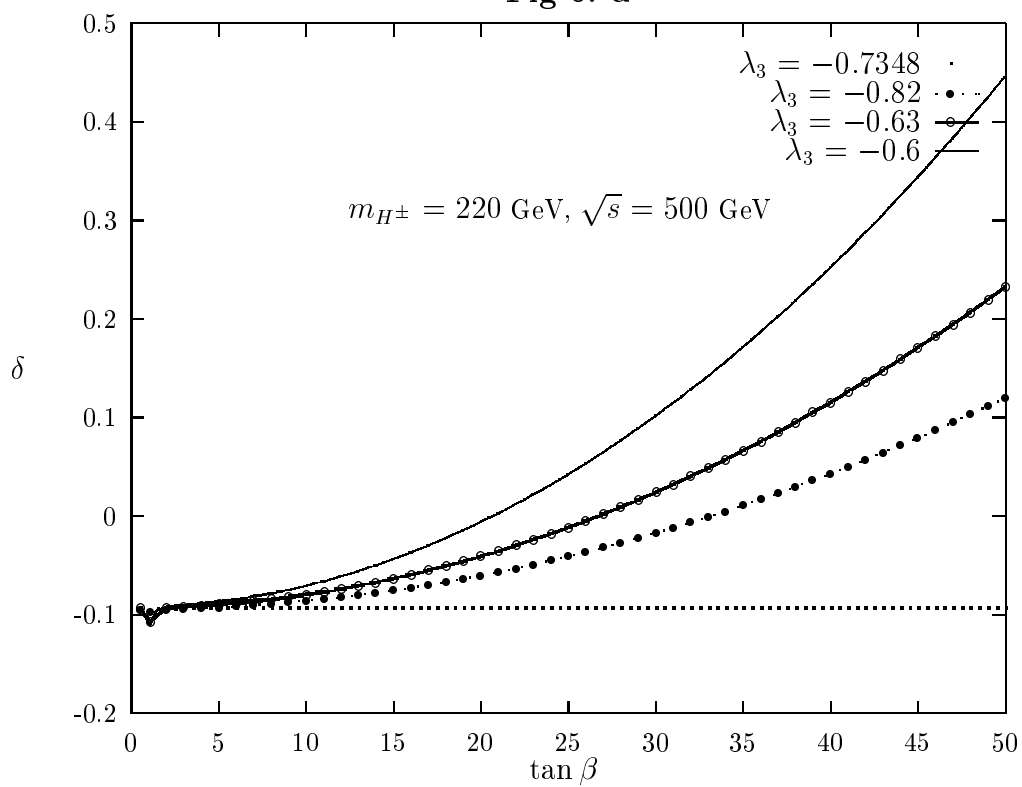


Fig 6. b

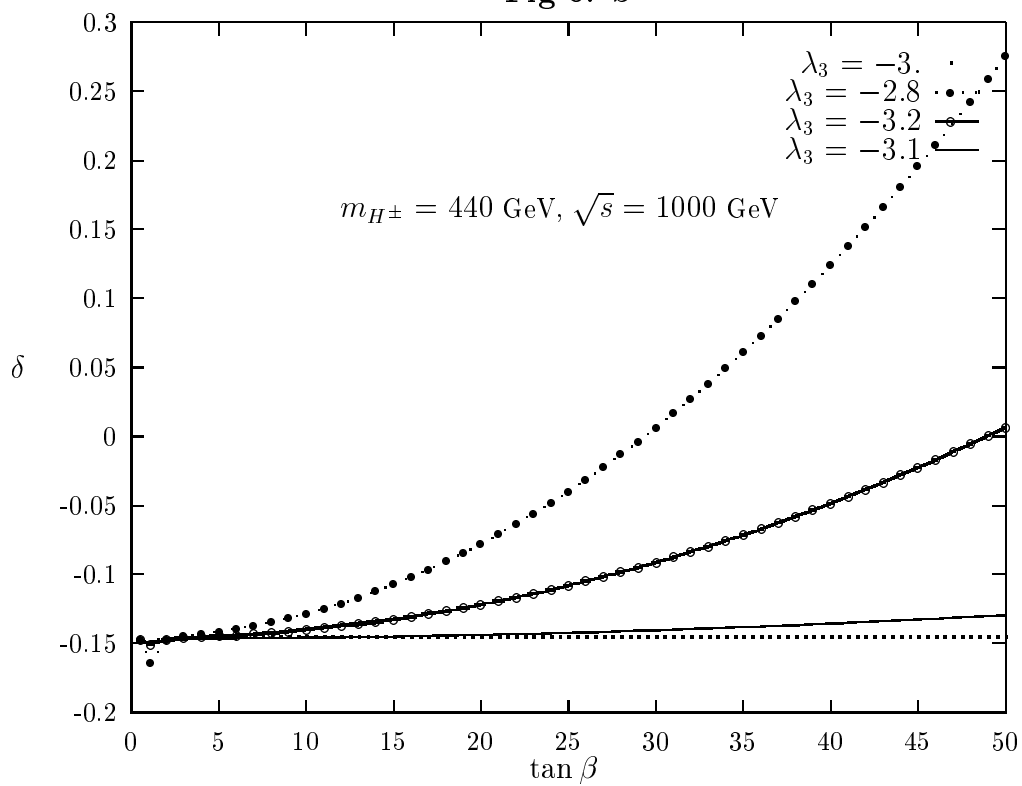


Figure. 6

Fig 6. c

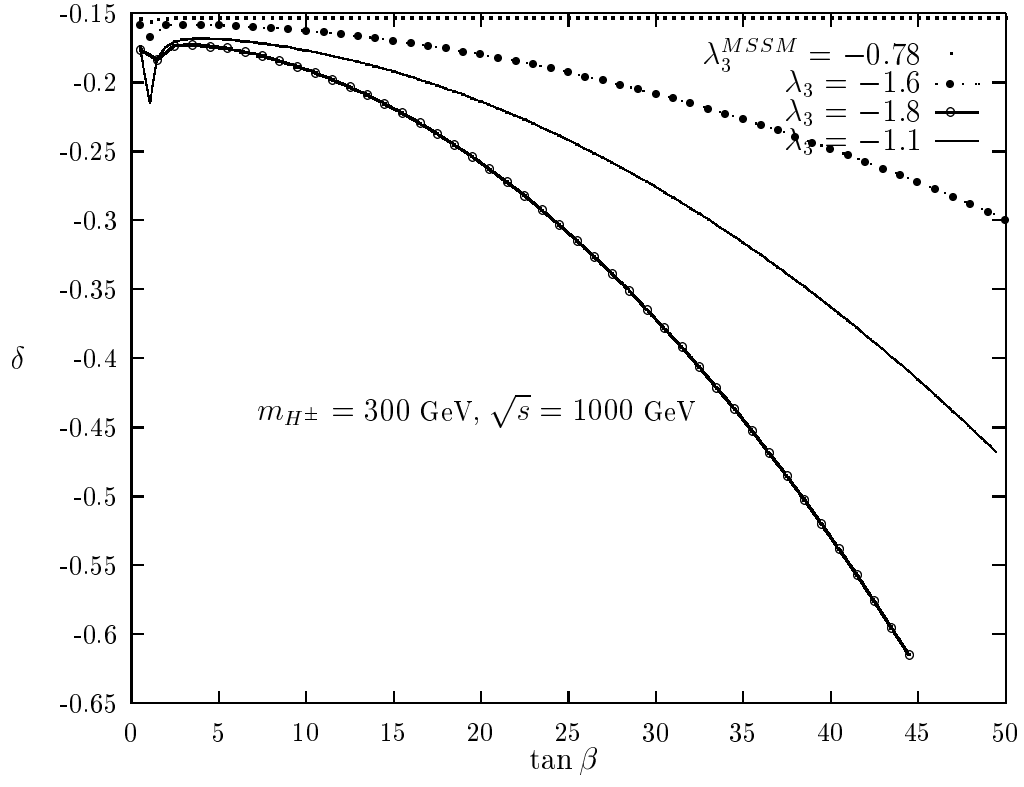


Figure. 6 (cont.)

Fig 7.

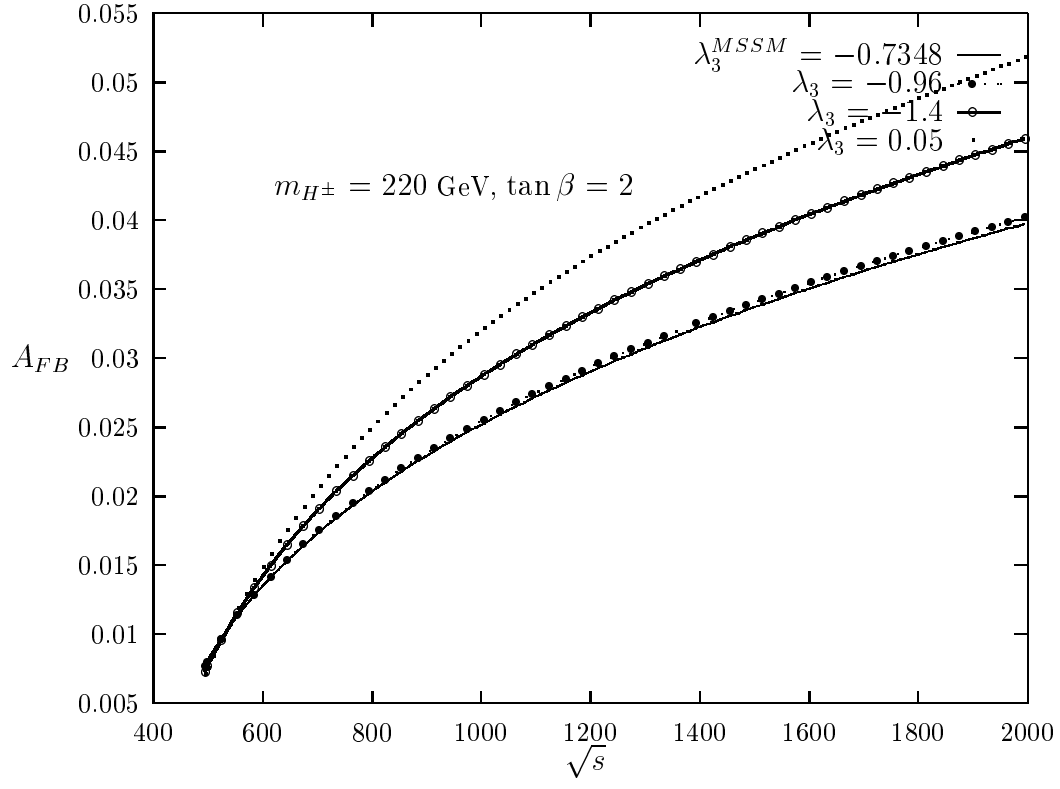


Figure. 7

Fig. 8. a

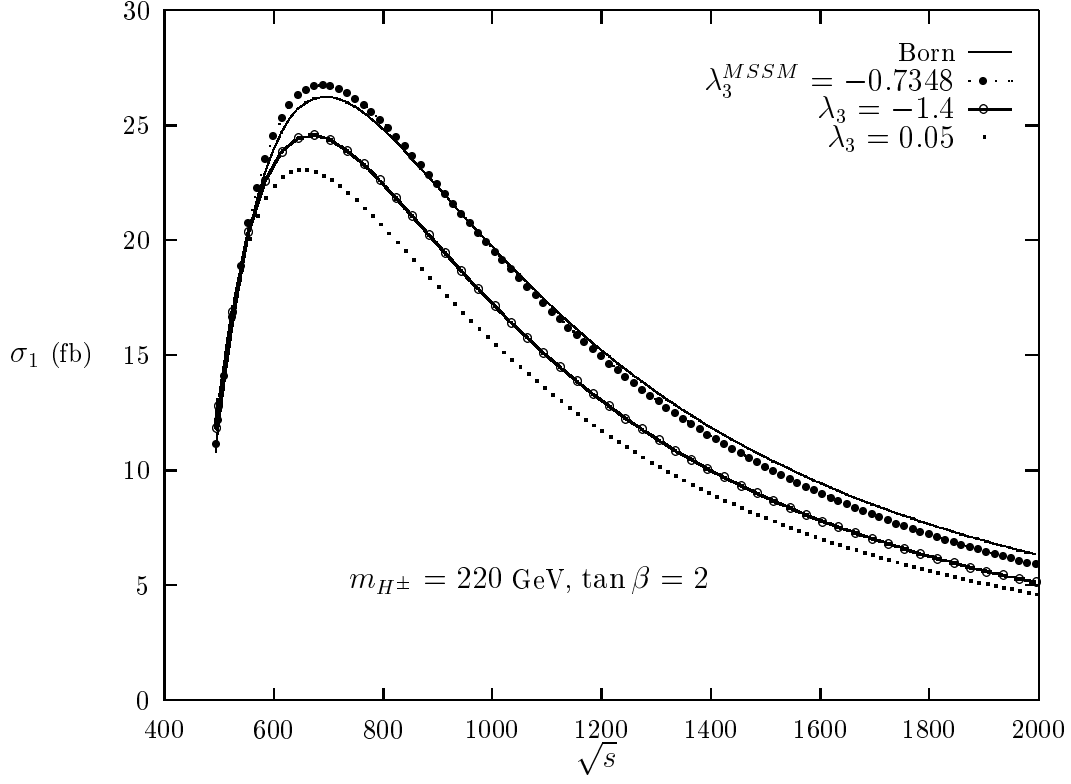


Fig. 8. b

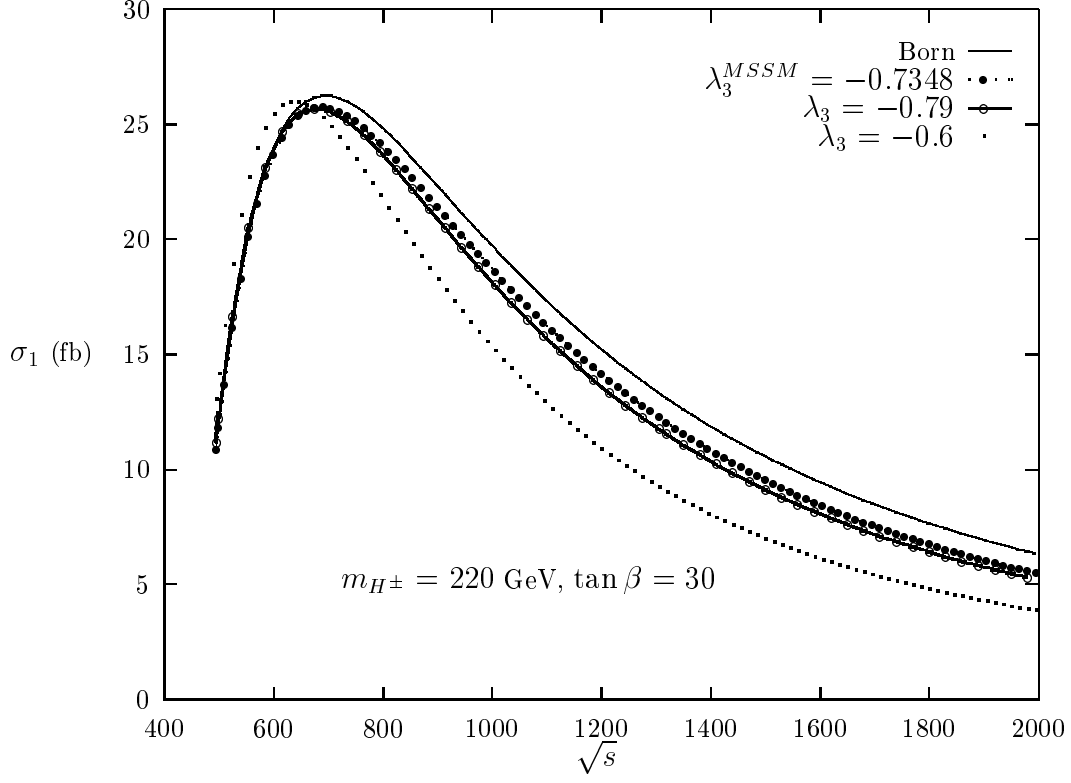


Figure. 8

Fig. 9. a

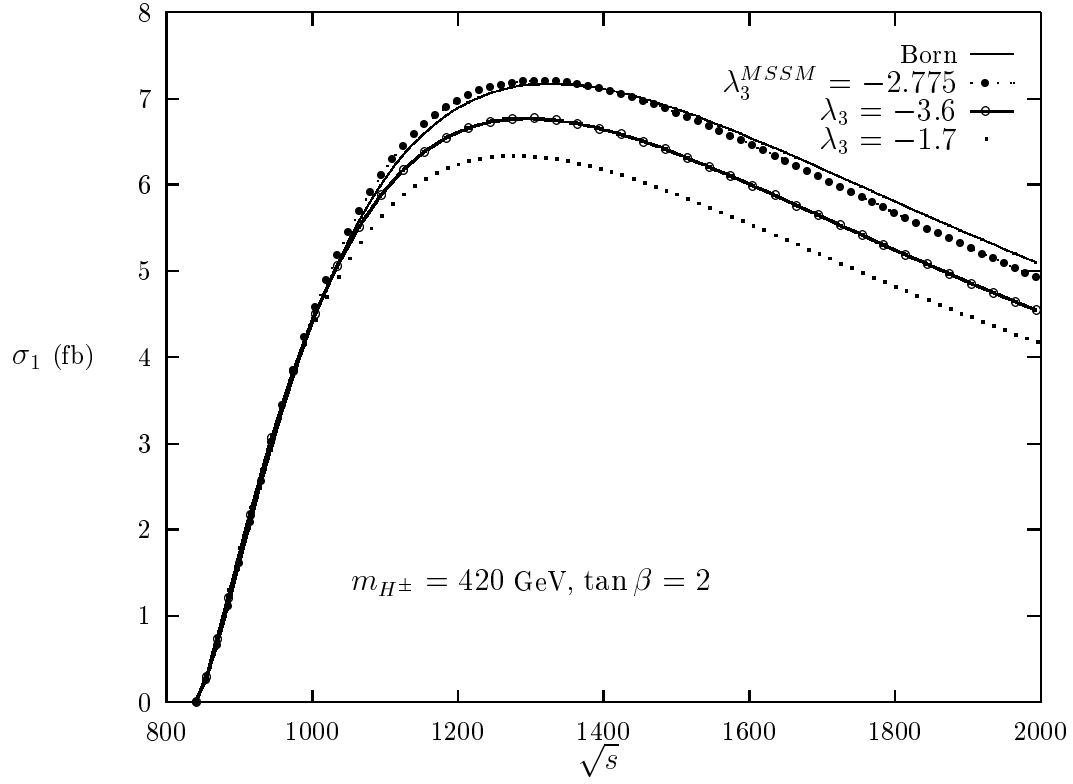


Fig. 9. b

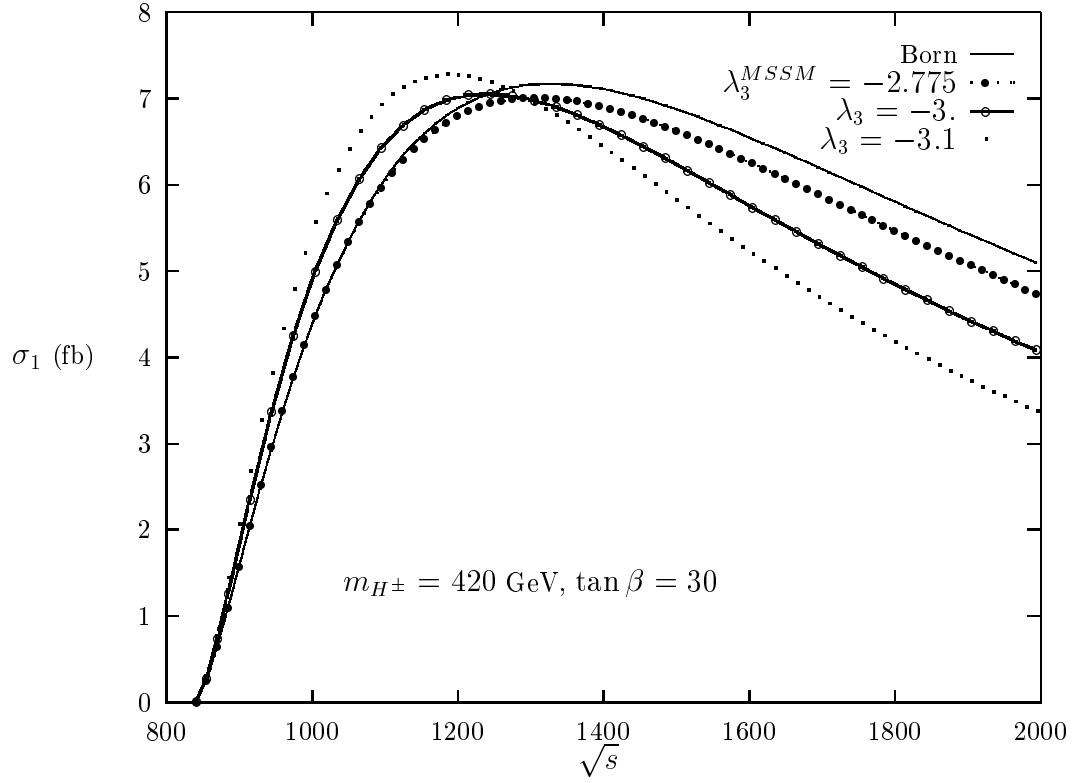


Figure. 9